

On asymmetric vortex pair interactions in shear

Patrick J.R. Folz^{1,†} and Keiko K. Nomura¹

¹Department of Mechanical and Aerospace Engineering, University of California, San Diego, 9500 Gilman Drive, La Jolla, CA 92093-0411, USA

(Received 6 November 2022; revised 10 April 2023; accepted 13 June 2023)

This study examines the two-dimensional interaction of two unequal co-rotating viscous vortices in uniform background shear. Numerical simulations are performed for vortex pairs having various circulation ratios $\Lambda_0 = \Gamma_{1,0}/\Gamma_{2,0} = (\omega_{1,0}/\omega_{2,0})(a_{1,0}^2/a_{2,0}^2) \leq 1$, corresponding to different initial characteristic radii $a_{i,0}$ and peak vorticities $\omega_{i,0}$ of each vortex $i = 1, 2$, in shears of various strengths $\zeta_0 = \omega_S/\omega_{2,0}$, where ω_S is the constant vorticity of the shear. Two primary flow regimes are observed: separations ($\zeta_0 < \zeta_{sep} < 0$), in which the vortices move apart continuously, and henditions ($\zeta_0 > \zeta_{sep}$), in which the interaction results in a single vortex (where ζ_{sep} is the adverse shear strength beyond which separation occurs). Vortex motion and values of $\zeta_{sep}(\Lambda_0)$ are well-predicted by a point-vortex model for unequal vortices. In vortex-dominated henditions, shear varies the peak–peak distance b , and vortex deformation. The main convective interaction begins when core detrainment of one vortex is established, and proceeds similarly to the no-shear ($\zeta_0 = 0$) case: merger occurs if the second vortex also detrains, engendering mutual entrainment; otherwise straining out occurs. Detrainment requires persistence of straining of both sufficient magnitude, as indicated by relative straining above a consistent critical value, $(S/\omega)_i > (S/\omega)_{cr}$, where S is the strain rate magnitude at the vorticity peak, and conducive direction. Hendition outcomes are assessed in terms of an enhancement factor $\varepsilon \equiv \Gamma_{end}/\Gamma_{2,start}$. Although ε generally varies with ζ_0 , $(a_{1,0}^2/a_{2,0}^2)$ and $(\omega_{1,0}/\omega_{2,0})$ in a complicated manner, this variation is well-characterized by the pair's starting enstrophy ratio, Z_2/Z_1 . Within a transition region between merger and straining out (approximately $1.65 < Z_2/Z_1 < 1.9$), shear of either sense may increase ε .

Key words: vortex dynamics, vortex interactions

† Email address for correspondence: pjfolz@ucsd.edu

1. Introduction

Vortices and their interactions play significant roles in myriad flows ranging from the astrophysical (Fu *et al.* 2014) to the quantum mechanical (Baggaley & Barenghi 2018), and as such, have attracted intense research interest for decades. A large portion of this research has focused on the relatively simplified case of two-dimensional vortices, which are generally agreed to play a role in the famous inverse energy cascade in two-dimensional turbulence, although by what means and to what extent remain uncertain (Xiao *et al.* 2009; Burgess, Dritschel & Scott 2017a,b; Sutyurin 2019). Studies of two-dimensional vortices and their role in inter-scale flow phenomena have generally fallen into one of two categories: macroscopic studies of the vortex population in aggregate, which generally focus on the evolution of the number of vortices in the flow field and the distribution of their properties (Tabeling 2002); and atomic studies that consider in detail a single pair of vortices, whose interaction is often considered a ‘building block’ of the more complicated flows (Lewke, Le Dizès & Williamson 2016). The vast majority of these atomic studies have considered a symmetric pair – two identical vortices – interacting in isolation; a handful have considered unequal vortices interacting in isolation; a small number have considered a symmetric pair in a background flow such as linear shear; and to date none have considered the most general case of two unequal vortices interacting in background flow. This is despite that last-mentioned case being, self-evidently, the most common in turbulent flows; to study it necessitates a robust, general understanding of the isolated two-vortex interaction, which until recently has remained elusive. However, recent developments have elucidated a general underlying physical model for vortex interactions, enabling the more general case to now be considered.

An isolated symmetric pair of two-dimensional co-rotating vortices undergoes merger, combining the fluid of each into a single compound vortex, when its aspect ratio surpasses a critical value, $a/b > (a/b)_{cr}$, where a is the characteristic vortex radius, and b is the peak–peak distance; prior to the onset of the merging process, $a = a(t)$ grows (in viscous flow) and $b = b_0$ remains constant (see e.g. Melander, Zabusky & McWilliams 1988; Cerretelli & Williamson 2003; Meunier, Le Dizès & Lewke 2005). This critical distance corresponds to the point at which their mutual strain causes the vortices to become sufficiently deformed that fluid detrains from the vortex cores, in the vicinity of a central hyperbolic point in the instantaneous streamline pattern (e.g. Velasco Fuentes 2005; Brandt & Nomura 2006). This engenders a mutual entrainment process whereby the vortex cores move together rapidly, producing the compound vortical structure (Huang 2005; Brandt & Nomura 2007). When viscosity is present, the continuous growth of a ensures that $(a/b)_{cr}$ is always eventually met (Melander *et al.* 1988).

An isolated asymmetric pair – two unequal co-rotating vortices – on the other hand, may interact in one of several different ways, depending on a number of factors (e.g. Melander, Zabusky & McWilliams 1987; Dritschel & Waugh 1992; Yasuda & Flierl 1997; Trieling, Velasco Fuentes & van Heijst 2005). There is therefore no simple critical merging distance or similar criterion for interaction (Dritschel & Waugh 1992). When viscosity is present, the interaction always produces a single vortex, but the interaction may be either a merger similar to the symmetric case, or a straining out in which only one vortex is induced to detrain and is ultimately broken up and destroyed, while the survivor remains essentially unaffected (Huang 2006). Thus the outcome of interaction depends upon the relative timing of detrainment and destruction (Brandt & Nomura 2010): once the first vortex is induced to detrain, if it can induce the second to also detrain before the first breaks up, then mutual entrainment ensues (i.e. merger occurs); otherwise, the first-detraining vortex is simply destroyed (i.e. straining out occurs).

In other words, the outcome of an asymmetric pair interaction derives from the degree of mutuality of the interaction. Folz & Nomura (2017) assessed these outcomes quantitatively in terms of an enhancement factor $\varepsilon \equiv \Gamma_{end}/\Gamma_{2,start}$ and a merging efficiency $\eta \equiv \Gamma_{end}/\Gamma_{tot,start}$, and found that all interaction outcomes across a wide range of pair parameters (including initial peak vorticity ratio $\omega_{1,0}/\omega_{2,0}$ and initial radius ratio $a_{1,0}/a_{2,0}$) were well-characterized by a mutuality parameter

$$MP = \frac{(S/\omega)_1}{(S/\omega)_2}, \tag{1.1}$$

which compares the relative straining $(S/\omega)_i$ of each vortex $i = 1, 2$, where S is the strain rate magnitude (note that $S = \sqrt{\mathbf{S}^2}$, where $\mathbf{S}^2 = \text{tr}[\mathbf{S}_{mn}\mathbf{S}_{mn}]$), and ω is the absolute vorticity at the vortex peak. Merger corresponds to MP near unity and straining out to high MP , with a narrow transition region between them. This is consistent with an earlier finding by Trieling *et al.* (2005) that the occurrence of complete merger of an asymmetric pair (in inviscid flow) was characterized reasonably well by a critical merging distance based on the pair’s mean radius (\bar{a}), while complete straining out occurred when b_0 was below that associated with an induced relative strain rate sufficient to cause breakup of a single vortex in shear. Dritschel & Waugh (1992) found similar results for highly disparate Rankine vortices. The relative straining, in turn, reflects the deformation (i.e. eccentricity) of each vortex (see Le Dizès & Laporte 2002; Leweke *et al.* 2016), and the onset of detrainment for a given vortex is associated with a consistent critical value $(S/\omega)_{cr} \approx 0.135 \pm 0.003$ (Folz & Nomura 2017). For a symmetric pair, these criteria are equivalent to $(a/b)_{cr}$. This mutuality model (including the detrainment–entrainment processes) constitutes a general model for the interaction of two two-dimensional vortices in isolation.

This paper now examines the influence of linear background shear – which can be considered a first-order approximation of the flow generated by surrounding vortices in a turbulent flow field – on these processes (e.g. Trieling, Dam & van Heijst 2010). The shear is characterized in terms of a shear strength parameter of the form

$$\zeta \equiv \omega_S/\omega_2, \tag{1.2}$$

which compares the constant vorticity of the shear $\omega_S = -\alpha \equiv -dU/dy$ to a characteristic vorticity of the pair (which potentially could be time-varying; here the vorticity of the stronger vortex 2 is used). Shear is considered favourable when it has the same rotational sense as the vortices, i.e. when $\zeta > 0$, and adverse when they are opposed, i.e. when $\zeta < 0$. In general, shear deforms a vortex elliptically, with the major axis oriented approximately orthogonal to or aligned with the shear direction in favourable and adverse shear, respectively.

When adverse shear acts on a single isolated vortex, the opposing rotations of the vortex and the shear create a pair of hyperbolic stagnation points in the elliptical streamline pattern about the vortex center, which causes peripheral vorticity of a non-uniform vortex to be advected away, or ‘stripped’, in the form of filaments (see e.g. Legras & Dritschel 1993; Kimura & Herring 2001; Legras, Dritschel & Caillol 2001; Hurst *et al.* 2016). This is fundamentally the same physical process as detrainment of a vortex in a pair. Increasing the relative strength of adverse shear (i.e. making $\zeta < 0$ more negative) causes detrainment to occur at progressively higher vorticity levels within the non-uniform vortex (Legras & Dritschel 1993), until a generally consistent critical shear strength is reached at which the vortex breaks up and is rapidly elongated into a filament ($\zeta_{bu} = -0.10$ to -0.13 ; see

also Mariotti, Legras & Dritschel 1994; Paireau, Tabeling & Legras 1997). In viscous flow, the peak vorticity of the vortex, $\omega = \omega(t)$, generally decays in time due to viscous diffusion, causing $|\zeta|$ (of either sense) to increase (as $\sim 1/\omega$, due to conservation of circulation $\Gamma = \pi a^2 \omega = \text{const.}$ as area increases, linearly for the no-shear, i.e. $\zeta_0 = 0$, case, $a^2(t) = a_0^2 + 4\nu t$; see e.g. Meunier *et al.* 2002), ensuring that detrainment and breakup always ultimately occur in adverse shear.

When two co-rotating vortices are present, the shear exerts these same influences directly upon each as they interact with each other. As noted above, all studies of this case to date have considered a symmetric pair (e.g. Carton, Maze & Legras 2002; Perrot & Carton 2010; Marques Rosas Fernandes *et al.* 2016). Additionally, and perhaps most significantly, sufficiently adverse shear, i.e. $\zeta < \zeta_{sep}$, causes separation of the pair, wherein the vortices simply move apart indefinitely rather than merging or orbiting (observed by Kimura & Hasimoto (1985) for point vortices; Maze, Carton & Lapeyre (2004) for finite-area inviscid vortices; and Folz & Nomura (2014) for finite-area vortices with viscosity). If it does not cause separation, the shear causes the vortices to follow elliptical trajectories rather than circular. Note that whether the shear causes $b = b(t)$ to increase or decrease from the initial b_0 depends not only upon the relative sense of shear, as is often stated in the literature, but also upon the initial orientation of the vortices (this is discussed briefly in § 5). In inviscid flow, a stationary case ($\zeta = \zeta_{sep}$) exists between the separation and elliptical motion cases, with two distinct types of cases for $\zeta > \zeta_{sep}$: periodic motion and merger. The occurrence of merger is found to be reasonably well-characterized by the minimum b falling sufficiently low that the aspect ratio surpasses the critical value previously found for symmetric pairs without shear (Trieling *et al.* 2010). In viscous flow, the presence of viscosity effectively ensures that merger always occurs when $\zeta > \zeta_{sep}$, commencing when the combined variation of a and b results in $a/b > (a/b)_{cr}$, where the value of $(a/b)_{cr}$ is similar to that observed in the no-shear case (Folz & Nomura 2014). In these cases, the primary effect of shear is to accelerate or delay the onset of the merging process.

Drawing upon these observations, the convective interaction of two unequal vortices under the influence of linear background shear is now examined. Numerical simulations of an asymmetric pair of two-dimensional viscous vortices in linear background shear are performed. The interaction regimes are identified and supported by analytical and point-vortex results. This study focuses primarily on cases in which the vortices interact to produce a single resulting vortex, i.e. henditions (see § 1.1). For these cases, the influence of shear on vortex motion, deformation and interaction processes is examined both qualitatively and quantitatively. A characterization of the interaction outcomes is developed, in the course of which a quantitative assessment is performed in the manner of Folz & Nomura (2017), and the results are correlated to significant pair parameters. Since the parameter space of this flow is quite large, this study considers primarily the effects of initial shear strength ζ_0 and initial circulation ratio Λ_0 , with two sub-categories of the latter. These results elucidate the major effects of shear on a pair of interacting vortices, and show how their interaction outcomes relate to the considered initial flow parameters, forming a basis from which future studies may consider further parameters and flow regimes.

This paper is organized as follows. First, § 2 discusses the motion of a pair of unequal point vortices in linear background shear, and an analytical expression for the critical shear strength for separation is obtained. Next, § 3 describes the flow set-up and simulations. Then § 4 gives general observations for vortex interactions in shear and identifies the main flow regimes: § 4.1 discusses separations, and § 4.2 outlines the vortex-dominated regime.

In § 5 is the heart of the study, which analyses vortex-dominated henditions. The first subsection, § 5.1, describes the method used to perform the quantitative assessment of the hention outcomes; the second subsection, § 5.2, examines the influence of the shear on the timing and duration of detrainment; and the final subsection, § 5.3, presents the results of the quantitative assessment and discusses the influence of shear. Finally, § 6 summarizes the findings, and discusses some implications and potential areas of further study. Supplementary material is also provided (available online at <https://doi.org/10.1017/jfm.2023.525>), which includes additional information about the quantities used to evaluate hentions, including their time development in the single-vortex case.

1.1. *A note on nomenclature: hention*

There is no extant word in the English language that means, simply, ‘two things become one thing’ without also implying either increase or enhancement (combination, unification, consolidation, fusion, incorporation, etc.). This is certainly the case for ‘merger’, which is used as a generic term by some researchers (e.g. Melander *et al.* 1987; Tabeling 2002; Jing, Kanso & Newton 2012), while others use it to denote specifically interactions that produce an enhanced resulting vortex (e.g. Dritschel & Waugh 1992; Trieling *et al.* 2005; Brandt & Nomura 2010). Other terms imply only destruction without any increase or enhancement (annihilation, removal, etc.). This muddles the terminology and obscures the distinction between fundamentally different types of interaction (those in which mutual entrainment does, and does not, occur).

As such, the authors introduce the new term ‘hention’, from the Greek phrase ‘ἓν διὰ δύοῖν’ meaning ‘one through two’. A hention is an occurrence in which there are two vortices at the start and only one at the end, regardless of the properties of the resulting vortex (relative to the starting vortices) or the physical process by which this interaction proceeds. Merger and straining out are then specific types of hention, as is the case of two vortices becoming one through diffusion (not considered here). In a more complicated flow, such as two-dimensional turbulence, the case of a dipole encountering a third vortex, after which the two like-signed vortices interact to produce one, would be considered a hention. The case of three or more like-signed vortices interacting simultaneously, resulting ultimately in a single vortex, could be referred to by a similar term: henmultion. It is hoped that the use of the term ‘hention’ will ensure clarity of this paper, and more generally may be of use in vortex-related discussions going forward.

2. Modified point-vortex model for unequal vortices

The basic behaviour of two well-separated vortices is similar to that of two point vortices (Trieling *et al.* 2010), even in viscous flow (Folz & Nomura 2014). Kimura & Hasimoto (1985) studied the motion of equal point vortices in shear, and Ryzhov, Koshel & Carton (2012) studied the motion of unequal point vortices in an arbitrary deformation flow. Here, the motion of two unequal point vortices in uniform background shear is examined, and the boundary between the major flow regimes is identified.

Two point vortices having circulation ratio $\Lambda \equiv \Gamma_1/\Gamma_2$ are located initially at $x_1 = -b_0/2$ and $x_2 = b_0/2$ and $y_0 = 0$, where b_0 is the initial peak–peak distance, and x and y are the flow and shear directions, respectively. The linear background shear has constant strength $\alpha \equiv dU/dy$. The vortices’ motion is described by a system of equations (Kimura

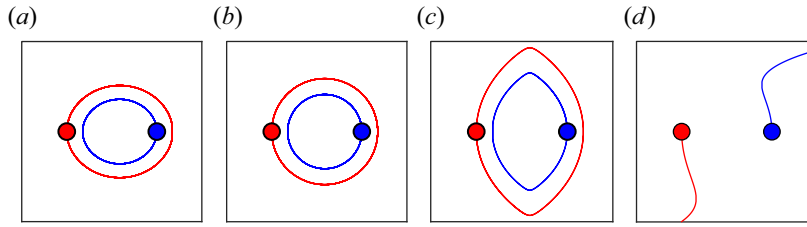


Figure 1. Trajectories of point vortices of pairs (red for vortex 1, blue for vortex 2), having circulation ratio $\Lambda = \Gamma_1/\Gamma_2 = 0.70$, within shear of various strengths $\mu = \alpha b_0^2/\Gamma_2$. For this case, separation shear strength is $\mu_{sep} = 0.0995$. The filled circles indicate the starting positions for the integrated trajectories (2.1)–(2.4), with (a) $\mu = -0.0992$, (b) $\mu = 0$, (c) $\mu = 0.0992$, and (d) $\mu = 0.128$.

& Hasimoto 1985)

$$\frac{dx_1}{dt} = -\frac{\Gamma_2}{2\pi} \frac{y_1 - y_2}{b^2} + \alpha y_1, \tag{2.1}$$

$$\frac{dy_1}{dt} = \frac{\Gamma_2}{2\pi} \frac{x_1 - x_2}{b^2}, \tag{2.2}$$

$$\frac{dx_2}{dt} = -\frac{\Gamma_1}{2\pi} \frac{y_2 - y_1}{b^2} + \alpha y_2, \tag{2.3}$$

$$\frac{dy_2}{dt} = \frac{\Gamma_1}{2\pi} \frac{x_2 - x_1}{b^2}, \tag{2.4}$$

where (x_i, y_i) are the coordinates of vortex $i = 1, 2$, and the instantaneous peak–peak distance $b = \sqrt{(x_1 - x_2)^2 + (y_1 - y_2)^2}$ may vary in time. The y-coordinate of the centre of rotation of the system is $Y = (\Gamma_1 y_1 + \Gamma_2 y_2)/(\Gamma_1 + \Gamma_2)$, and is always at 0.

These equations can be integrated to find the vortex trajectories. In symmetric flow, these trajectories are either closed or open, with a critical stationary case separating these regimes (Kimura & Hasimoto 1985). Trieling *et al.* (2010) characterized these regimes using a non-dimensional shear strength parameter $\mu_s = \alpha b_0^2/\Gamma$ for symmetric vortices. Closed trajectories occur in favourable ($\mu_s < 0$) to weakly adverse ($\mu_{s,sep} > \mu_s > 0$) shear, where $\mu_{s,sep}$ is the critical shear strength associated with the stationary case. In this regime, from their initial position, the vortices follow overlapping elliptical trajectories where an extremum of b occurs when the vortices are aligned vertically, i.e. along the shear direction. This extremum is minimum b in favourable shear, and maximum b in adverse shear, respectively, with circular trajectories occurring in the no-shear case ($\mu_s = 0$). Open trajectories occur in strongly adverse shear ($\mu_s > \mu_{s,sep} > 0$), and the vortices simply move apart continuously; this behaviour is termed separation.

For the case of unequal vortices, a similar parameter is constructed:

$$\mu = \alpha b_0^2/\Gamma_2 \tag{2.5}$$

based on the stronger vortex, here taken to be 2. Figure 1 shows example trajectories for a pair having $\Lambda = 0.70$ in various μ . Similar regimes are observed, with the vortices following closed concentric elliptical trajectories for favourable ($\mu < 0$) or weakly adverse ($\mu_{sep} > \mu > 0$) shear, and open trajectories for strongly adverse shear ($\mu > \mu_{sep}$), distinguished by a critical separation shear strength μ_{sep} .

In the symmetric case, an analytical expression for the critical shear strength associated with the stationary case, similar to $\mu_{s,sep}$, was derived by Kimura & Hasimoto (1985)

using the Hamiltonian of the system (2.1)–(2.4),

$$H = \frac{-\Gamma_1\Gamma_2}{4\pi} \ln[(x_1 - x_2)^2 + (y_1 - y_2)^2] + \frac{\alpha}{2}(\Gamma_1y_1^2 + \Gamma_2y_2^2). \quad (2.6)$$

When the vortices are unequal, many of their simplifying assumptions cannot be made, but an analytical expression for μ_{sep} may nevertheless be found in the following manner.

Rearranging (2.6) gives

$$H - \frac{\alpha}{2}(\Gamma_1y_1^2 + \Gamma_2y_2^2) = \frac{-\Gamma_1\Gamma_2}{4\pi} \ln[(x_1 - x_2)^2 + (y_1 - y_2)^2]. \quad (2.7)$$

Then

$$\exp\left(H \frac{-4\pi}{\Gamma_1\Gamma_2} - \frac{-4\pi}{\Gamma_1\Gamma_2} \frac{\alpha}{2}(\Gamma_1y_1^2 + \Gamma_2y_2^2)\right) = ((x_1 - x_2)^2 + (y_1 - y_2)^2), \quad (2.8)$$

and noting that H is constant,

$$C \exp\left(\frac{4\pi}{\Gamma_1\Gamma_2} \frac{\alpha}{2}(\Gamma_1y_1^2 + \Gamma_2y_2^2)\right) = ((x_1 - x_2)^2 + (y_1 - y_2)^2) = \xi^2 + \eta^2, \quad (2.9)$$

where $\xi \equiv x_1 - x_2$ and $\eta \equiv y_1 - y_2$ (using the nomenclature of Kimura & Hasimoto 1985), and $C = \xi_0^2$ since $\eta = 0$ in the initial condition.

When the vortices are oriented vertically, the coordinates y_1 and y_2 are equal to the distances of the weaker and stronger vortices from the centre of rotation, r_1 and r_2 respectively, since that centre remains fixed in space. Additionally, $\eta = b$ in the vertical orientation. Therefore, at the critical time,

$$y_1 = r_1 \equiv \frac{1}{1 + \Lambda} \eta_v, \quad y_2 = r_2 \equiv \frac{\Lambda}{1 + \Lambda} \eta_v, \quad (2.10a,b)$$

where η_v is η when the vortices are aligned vertically, and $\Lambda \equiv \Gamma_1/\Gamma_2$. So

$$\xi_0^2 \exp\left(\frac{2\pi\alpha}{\Gamma_1\Gamma_2}(\Gamma_1r_1^2 + \Gamma_2r_2^2)\right) = \eta_v^2, \quad (2.11)$$

$$\xi_0^2 \exp\left(\frac{2\pi\alpha}{\Lambda\Gamma_2}\left(\Lambda \frac{\eta_v^2}{(1 + \Lambda)^2} + \frac{\Lambda^2\eta_v^2}{(1 + \Lambda)^2}\right)\right) = \eta_v^2, \quad (2.12)$$

and ultimately

$$\xi_0^2 \exp\left(\frac{2\pi\alpha}{\Gamma_2(1 + \Lambda)} \eta_v^2\right) = \eta_v^2. \quad (2.13)$$

Normalizing (2.13) by the initial peak–peak distance $\xi_0 = b_0$,

$$\exp\left(\frac{2\pi\alpha b_0^2}{\Gamma_2(1 + \Lambda)} \left(\frac{\eta_v}{b_0}\right)^2\right) = \left(\frac{\eta_v}{b_0}\right)^2. \quad (2.14)$$

For this equation to have a finite solution, it must be true that

$$\frac{2\pi\alpha b_0^2}{\Gamma_2(1 + \Lambda)} \leq \frac{1}{e}, \quad (2.15)$$

Λ_0	$a_{1,0}^2/a_{2,0}^2$	$\zeta_{sep,p}$	ζ_{sep}	
			$Re_\Gamma = 5000$	$Re_\Gamma = 1000$
1.0	1.0	-0.0091	-0.0093 ± 0.0001	-0.0093 ± 0.0001
0.9	1.0	-0.0086	-0.0089 ± 0.0002	-0.0089 ± 0.0002
0.8	1.0	-0.0082	-0.0084 ± 0.0002	-0.0084 ± 0.0002
0.7	1.0	-0.0077	-0.0077 ± 0.0002	-0.0079 ± 0.0001
0.6	1.0	-0.0073	-0.0074 ± 0.0001	-0.0074 ± 0.0001
0.5	1.0	-0.0068	-0.0069 ± 0.0001	—
0.9	0.9	-0.0086	-0.0089 ± 0.0002	-0.0089 ± 0.0002
0.8	0.8	-0.0082	-0.0084 ± 0.0002	-0.0084 ± 0.0002
0.7	0.7	-0.0077	-0.0077 ± 0.0002	-0.0080 ± 0.0002
0.6	0.6	-0.0073	-0.0074 ± 0.0001	-0.0074 ± 0.0001
1.0	0.9	-0.0091	-0.0093 ± 0.0002	—
1.0	0.6	-0.0091	-0.0093 ± 0.0003	—
0.9	0.81	-0.0086	-0.0086 ± 0.0002	—
0.9	0.54	-0.0086	-0.0088 ± 0.0002	—

Table 1. Predicted $\zeta_{sep,p}$ from (2.18), with corresponding observed $\zeta_{sep} = -\alpha/\omega_{2,0}$ from numerical simulation of various starting pairs having $a_{2,0}/b_0 = 0.157$ (see § 4.1). The margin of error on the empirical data corresponds to the bracketing values used to determine ζ_{sep} .

so the critical criterion in terms of $\mu = \alpha b_0^2/\Gamma_2$ is

$$\mu_{sep} = \frac{(1 + \Lambda)}{2\pi e}. \tag{2.16}$$

Note that for symmetric vortices, this is identical to the criterion found by Trieling *et al.* (2010).

This criterion can be modified to apply for well-separated finite area vortices. Recalling that each vortex’s circulation remains constant in this case, $\Gamma_2 = \Gamma_{2,0} = \pi a_{2,0}^2 \omega_{2,0}$ may be substituted into (2.16), where $a_{2,0}$ and $\omega_{2,0}$ are the stronger vortex’s initial characteristic radius and peak vorticity, respectively:

$$\mu_{sep} = (\alpha b_0^2/\pi a_{2,0}^2 \omega_{2,0})_{sep} = \frac{(1 + \Lambda)}{2\pi e}. \tag{2.17}$$

Then

$$\left(\frac{-\alpha}{\omega_{2,0}}\right)_{sep} \equiv \zeta_{sep,p} = \frac{-(1 + \Lambda)}{2e} \left(\frac{a_{2,0}}{b_0}\right)^2, \tag{2.18}$$

where $\zeta_{sep,p}$ is a critical shear strength for the separation of finite-area vortices as predicted by this modified point-vortex model (an equivalent expression can be found by normalizing using vortex 1). It is seen that there is direct dependence between the magnitude of $\zeta_{sep,p}$ and both Λ and $(a_{2,0}/b_0)$: a more disparate pair (i.e. having lower Λ) will separate for weaker adverse shear than a more similar pair, although there is a minimum adverse shear strength required for any separation to occur ($\lim_{\Lambda \rightarrow 0} \zeta_{sep,p}(\Lambda) = (a_{2,0}/b_0)^2/(2e) \neq 0$). Likewise, a given pair (i.e. having a given Λ) will separate for weaker shear the smaller their initial aspect ratio $a_{2,0}/b_0$ is (i.e. the larger their initial normalized peak–peak distance). Values for $\zeta_{sep,p}$ for various pairs are shown in table 1. In § 4.1, these values are compared to empirical results from simulations of finite-area pairs.

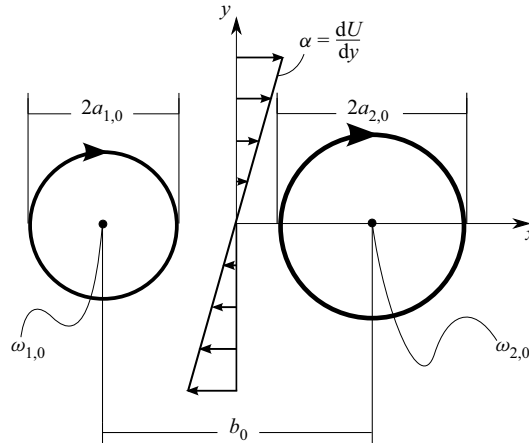


Figure 2. Initial flow configuration: two co-rotating vortices, $i = 1, 2$ (peak vorticity $\omega_{i,0}$, characteristic radius $a_{i,0}$, Gaussian vorticity distribution), whose peak–peak axis is oriented orthogonally to the direction of linear background shear (strength $\alpha = dU/dy$). The case shown has $\zeta_0 > 0$.

3. Set-up and numerical simulations

The initial flow configuration is shown in figure 2: for each case, two finite-area, co-rotating vortices are initially oriented along the flow direction of linear background shear, separated by an initial peak–peak distance b_0 . Each vortex $i = 1, 2$ is initially circular with a Gaussian vorticity distribution, and has an initial peak vorticity $\omega_{i,0}$ and characteristic radius $a_{i,0}$, giving an initial circulation ratio

$$\Lambda_0 \equiv \frac{\Gamma_{1,0}}{\Gamma_{2,0}} = \frac{\omega_{1,0}a_{1,0}^2}{\omega_{2,0}a_{2,0}^2} \leq 1. \quad (3.1)$$

This study focuses primarily on pairs having either $\omega_{1,0}/\omega_{2,0} < 1$, $a_{1,0}^2/a_{2,0}^2 = 1$ (termed ‘UPEA’ for ‘unequal peaks, equal areas’), or $\omega_{1,0}/\omega_{2,0} = 1$, $a_{1,0}^2/a_{2,0}^2 < 1$ (termed ‘EPUA’ for ‘equal peaks, unequal areas’), as well as symmetric pairs (i.e. those having $\omega_{1,0}/\omega_{2,0} = a_{1,0}^2/a_{2,0}^2 = 1$). A handful of pairs having $\omega_{1,0}/\omega_{2,0} \neq 1$, $a_{1,0}^2/a_{2,0}^2 \neq 1$ (termed ‘UPUA’ for ‘unequal peaks, unequal areas’) are also included in § 4.1. The overall range of circulation ratios considered is $0.6 \leq \Lambda_0 \leq 1$ (a few additional UPEA cases with $\Lambda_0 = 0.50$ were also performed to aid in the analysis of separations). The pair’s initial aspect ratio $a_{2,0}/b_0 = 0.157$ and the circulation Reynolds number $Re_\Gamma = \Gamma_{2,0}/\nu = 5000$ are maintained at constant values in order to facilitate comparison with the no-shear case ($\zeta_0 = 0$) examined previously in Folz & Nomura (2014, 2017). This also allows each vortex of the initially well-separated pair to adjust to the combined influence of the other vortex and the shear prior to interacting. This methodology helps to ensure that observed differences between the present results and the no-shear case are attributable primarily to the effects of shear.

The numerical simulations are performed using a hybrid finite-difference/pseudo-spectral code with periodic boundary conditions in the flow direction and shear-periodic boundary conditions in the shear direction (see Gerz, Schumann & Elghobashi (1989) for details of the method). The pair is initially positioned at the centre of a square domain of size $L \times L$ with 2048^2 grid points, and $b_0 = 1/24L$. This gives a resolution of approximately 38 points across the larger core. In comparison with a 1024^2 grid for cases

spanning the considered parameter range, differences in computed vortex quantities were found to be small (e.g. core circulation, an integrated quantity, differed by at most 2%, and the starting relative straining $(S/\omega)_1$, a pointwise quantity, differed by at most 5%), the quantitative assessments were similar (e.g. the merging efficiency η differed by at most five percentage points, and typically less than two; these quantities are discussed in § 5), and qualitatively all notable phenomena were observed for both resolutions in each case. Domain size independence was also tested using an initial separation distance $b_0 = 1/12L$ in the favourable case and $b_0 = 1/18L$ in the adverse case, with similarly small observed differences (e.g. η differed by at most six percentage points). The higher 2048² resolution and smaller $b_0 = 1/24L$ were utilized in all cases in order to minimize spurious variation in core quantities employing the threshold (see § 5), and to maintain maximum fidelity in general (this resolution was also previously found to be sufficient for the no-shear case; see Brandt & Nomura 2007, 2010).

The relative strength of the constant shear, $\alpha \equiv dU/dy$, is characterized in terms of its vorticity ω_s relative to that of the stronger vortex in the initial condition $\omega_{2,0}$:

$$\zeta_0 \equiv \frac{\omega_s}{\omega_{2,0}} = \frac{-\alpha}{\omega_{2,0}}. \tag{3.2}$$

In order to allow the vortices to adjust to the shear prior to the start of the main convective interaction, the range of $|\zeta_0|$ considered is limited to $|\zeta_0| < \zeta_{adj}$, where ζ_{adj} is a value chosen such that the viscous increase of $|\zeta|$ ($\sim 1/\omega(t)$; see § 1) would not be sufficient to induce detrainment prior to the end of the adjustment period of the vortices to each other, t_{adj}^* . This value ensures that $|\zeta_1(t_{adj}^*)|, |\zeta_2(t_{adj}^*)| < |\zeta_{cr,s}|$, where the critical shear strength associated with detrainment, $\zeta_{cr,s} \approx -0.063$, was found through simulations of a single vortex in shear (see the supplementary material). An estimate for t_{adj}^* is made using results from Le Dizès & Verga (2002) for a Gaussian vortex having $Re_\Gamma = 2000$ (the lower Re_Γ result is used to ensure a conservative estimate), which indicate an adjustment period of approximately $tv/(\pi a_{1,0}^2) = 0.05$ using their nomenclature. Using analytical results for a single isolated Gaussian vortex (see § 1) gives a requirement that $|\zeta_{i,0}| \leq 0.0387$, which in turn gives a value $|\zeta_{2,0}| \leq \zeta_{adj} \equiv 0.0387(\omega_{1,0}/\omega_{2,0})$.

In all cases, temporal results are presented on a convective time scale $t^* = t/T_0$, where $T_0 = (4\pi b_0^2)/(\Gamma_{1,0} + \Gamma_{2,0})$ is the period of revolution of a pair of point vortices having the same Λ_0 and $\zeta_0 = 0$.

4. General flow behaviour

First, observations of the general flow behaviour are made, and the major interaction regimes identified, for two unequal vortices interacting in the presence of shear (with finite viscosity). Figures 3 and 4 show vorticity contours of example cases demonstrating the major trends with respect to shear strength ζ_0 and vortex circulation ratio Λ_0 . Observations for UPEA and EPUA cases are qualitatively similar, so only UPEA cases are shown. The motion and full flow development of two illustrative cases, $\zeta_0 = 0.0167$, $\Lambda_0 = 0.90$ and $\zeta_0 = -0.0073$, $\Lambda_0 = 0.70$, can be seen in supplementary movies 1 and 2, with useful related information presented in figure 5.

For comparison, a no-shear merger case is included ($\zeta_0 = 0$, $\Lambda_0 = 0.90$, figure 3d) and reviewed briefly. As discussed in § 1, when shear is not present, the vortices initially (columns 1–4) revolve along concentric circular trajectories (maintaining constant peak–peak distance b_0 ; see dashed lines in figures 5b,e), growing by viscous diffusion and deforming elliptically along the peak–peak axis due to their intensifying mutually induced

Asymmetric vortex pairs in shear

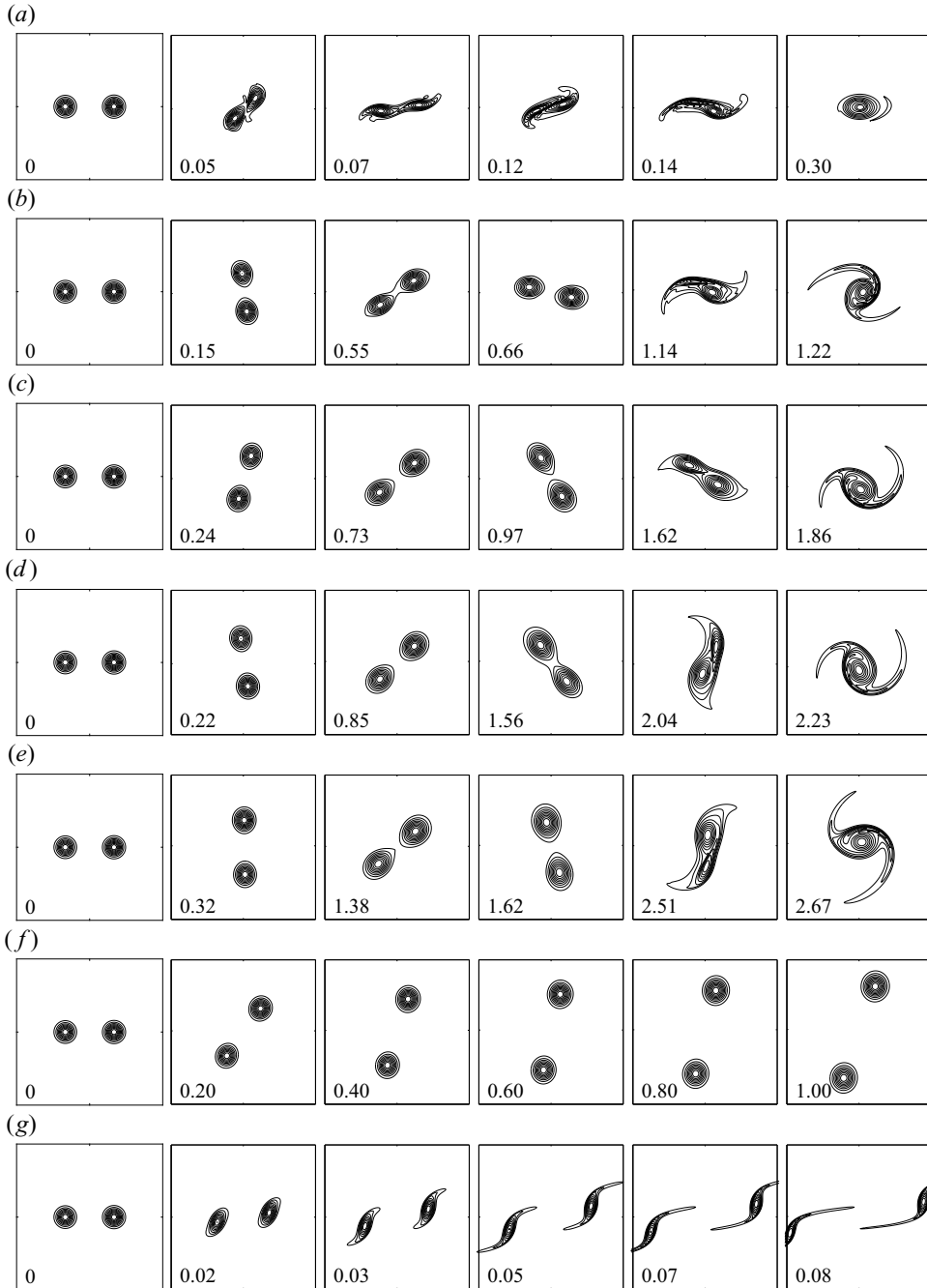


Figure 3. Vorticity contour plots showing time evolution of flows for UPEA pairs having $Re_\Gamma = 5000$ and $\Lambda_0 = 0.90$, with varying shear strength ζ_0 : (a) $\zeta_0 = 0.1$, (b) $\zeta_0 = 0.0167$, (c) $\zeta_0 = 0.0045$, (d) $\zeta_0 = 0$ (no shear), (e) $\zeta_0 = -0.0045$, (f) $\zeta_0 = -0.0091$, and (g) $\zeta_0 = -0.1$. For $\Lambda_0 = 0.90$, $\zeta_{sep} = -0.0089$ (see table 1) and $\zeta_{adj} = 0.0348$; cases (b–e) fall within the vortex-dominated regime, $\zeta_{sep} < \zeta_0 < \zeta_{adj}$. For these cases, each column corresponds to an equivalent stage of flow development (see §§ 4 and 5.2): column 1, initial condition; column 2, first quarter-turn; column 3, oriented approximately 45° above the positive x -axis; column 4, start of core detrainment, $t^* = t_{start}^*$; column 5, end of core detrainment and start of mutual entrainment, $t^* = t_{det}^*$; and column 6, end of mutual entrainment, $t^* = t_{ent}^*$. For cases (a, f, g), the column images have been chosen to illustrate the general flow development. The vortices rotate clockwise in favourable shear (counter-clockwise in adverse shear). The contour interval is 10%, and t^* for each plot is indicated at the lower left. The data in (d) were presented previously in Folz & Nomura (2017).

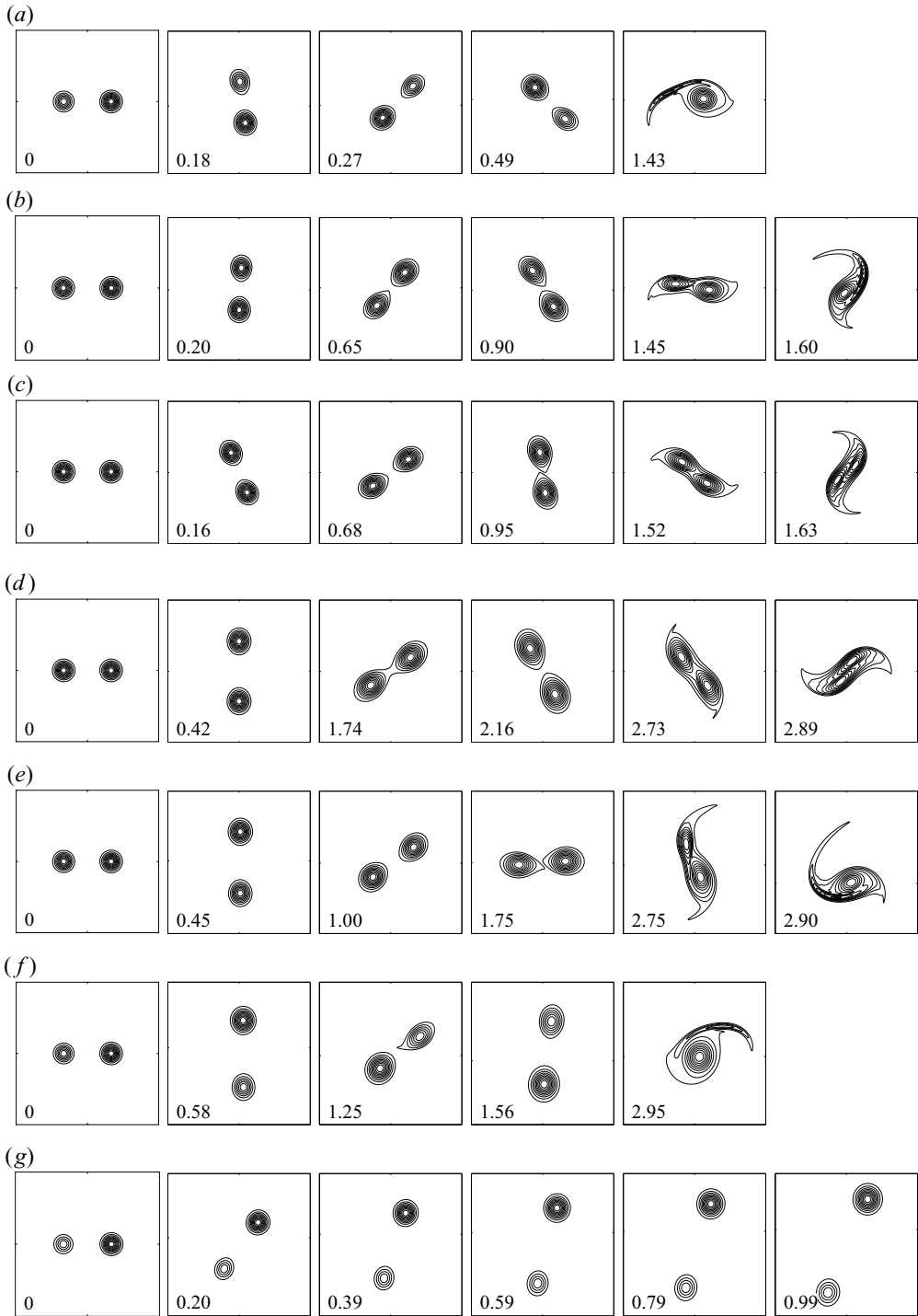


Figure 4. Vorticity contour plots showing time evolution of flows for UPEA pairs having $Re_\Gamma = 5000$ and $|\zeta_0| = 0.0073$, with varying Λ_0 : (a) $\Lambda_0 = 0.7$, (b) $\Lambda_0 = 0.9$, (c) $\Lambda_0 = 1.0$ having favourable shear ($\zeta_0 = 0.0073$); and (d) $\Lambda_0 = 1.0$, (e) $\Lambda_0 = 0.9$, (f) $\Lambda_0 = 0.7$, (g) $\Lambda_0 = 0.5$ having adverse shear ($\zeta_0 = -0.0073$). The columns have meanings equivalent to those in figure 3, but the sixth column of the straining out cases has been omitted since no entrainment occurs. The vortices rotate clockwise in favourable shear (counter-clockwise in adverse shear). The contour interval is 10 %, and t^* for each plot is indicated at the lower left.

Asymmetric vortex pairs in shear

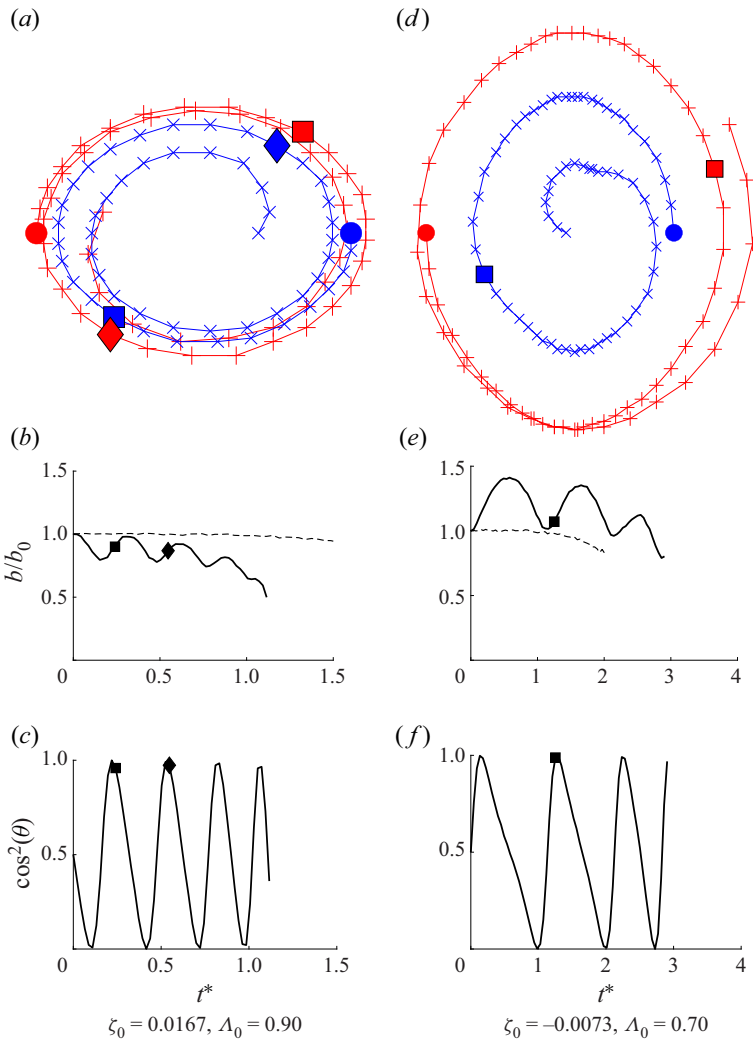


Figure 5. Time development of the vortex pair prior to the end of core detrainment for illustrative cases (solid lines): (a,d) trajectories of vortex peaks (red \times indicates vortex 1, blue $+$ indicates vortex 2); (b,e) normalized separation distance b/b_0 ; and (c,f) $\cos^2(\theta)$ of the angle θ between the peak–peak axis of the pair and the principal extensional strain eigenvector of the shear, \mathbf{e}_α , which is oriented 45° from the flow direction. The Reynolds number is $Re_T = 5000$. Filled circles indicate starting positions, a square indicates the time of the first deformation maximum prior to the start of detrainment, and a diamond indicates the second such maximum that occurs in the $\zeta_0 = 0.0167$, $\Lambda_0 = 0.90$ case. These times are taken at the corresponding local maxima in the relative straining of the weaker vortex in each case, $(S/\omega)_1$, as discussed in § 5.1. In (b,e), the dashed line corresponds to the no-shear case having the same Λ_0 .

strain, leading eventually to detrainment of at least one vortex’s core fluid in the vicinity of the centre of rotation (column 4). This is the start of the main convective interaction: if both vortex cores detrain (columns 4–5), then a two-way interaction with mutual entrainment (columns 5–6), i.e. merger, occurs (as in figure 3d); otherwise, one vortex detrains and breaks up while the other remains relatively unaffected, i.e. straining out occurs. Due to the presence of viscosity, all like-signed pair interactions without shear are henditions, i.e. they result in a single vortex.

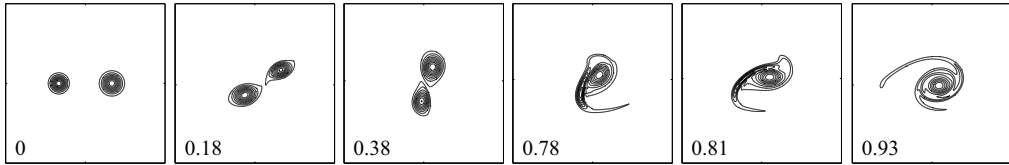


Figure 6. Vorticity contours for $\zeta_0 = 0.033$, $\Lambda_0 = a_1^2/a_2^2 = 0.70$, EPUA case (contour interval is 10 %, and $Re_T = 5000$). This case is a merger, whereas the equivalent no-shear case is a straining out (discussed further in § 5.1).

When shear is present ($\zeta_0 \neq 0$), it alters the motion and deformation of a pair (having a given Λ_0) in a manner and degree determined by its relative strength (figure 3). When shear is favourable ($\zeta_0 > 0$, figures 3a–c) or weakly adverse ($\zeta_{sep} < \zeta_0 < 0$, figure 3e), the interaction is a hendition; otherwise, when shear is strongly adverse ($\zeta_0 < \zeta_{sep} < 0$, figures 3f,g), the vortices undergo separation and move apart continuously. The separation case is discussed in § 4.1.

During shear-influenced henditions (such as those shown in the illustrative cases, i.e. figures 3(b) and 4(f) and supplementary movies 1 and 2), the vortices follow concentric elliptical trajectories in which the peak–peak distance b reaches a minimum (when $\zeta_0 > 0$) or maximum (when $\zeta_0 < 0$) when the peak–peak axis is aligned with the shear direction, akin to the point-vortex case discussed in § 2 (figures 5a,d,b,e). The shear causes periodic amplification of the deformation of the vortices, but, notably, this deformation is greatest when the peak–peak axis is oriented through the first and third quadrants, i.e. approximately along the direction of principal extensional strain of the shear, and not when b is minimal (figures 3a–c,e and 4a–f, columns 1–3, and figure 5). When shear is strongly favourable (figure 3a), it reduces b and amplifies deformation so substantially that it is the predominant cause of the hendition. Otherwise, when shear is weakly favourable or adverse, it is the viscous growth of the vortices and concomitant intensification of mutual strain that eventually cause detrainment to initiate and the main interaction to occur, similar to the no-shear case.

For a given shear strength ζ_0 , the circulation ratio of the pair, Λ_0 , influences whether the interaction is a hendition or a separation, and the type of hendition should one occur (figure 4). For a symmetric pair in weakly favourable or adverse shear (figures 4c,d), assuming $\zeta_0 > \zeta_{sep}(\Lambda_0 = 1.0)$ (recall from § 2 that $\zeta_{sep} = \zeta_{sep}(\Lambda_0)$), the interaction is a merger, similar to the no-shear case, but with the vortices experiencing equal shear-induced periodic amplification of deformation. For increasing asymmetry of the pairs (figures 4b–a,e–f), the variation of b increases, the deformation amplification becomes increasingly unequal (greater for the weaker), and during the main convective interaction, the mutual entrainment process becomes increasingly one-sided (e.g. the $\zeta_0 = 0.167$, $\Lambda_0 = 0.90$ illustrative case). When the pair is sufficiently disparate (figures 4a,f), the interaction is entirely one-sided and the weaker vortex is simply destroyed, leaving the stronger one essentially unaffected, i.e. straining out occurs (e.g. the $\zeta_0 = -0.0073$, $\Lambda_0 = 0.70$ illustrative case). In adverse shear, sufficiently small Λ_0 may result in $\zeta_0 < \zeta_{sep}(\Lambda_0)$ (unless $\zeta_0 > \zeta_{sep}(\Lambda_0 = 0)$), and separation may occur instead, i.e. asymmetry may in a sense ‘cause’ separation in certain circumstances.

Additionally, merger may occur in certain cases with higher $|\zeta_0|$ that for lower or zero $|\zeta_0|$ are straining out. An example is shown in figure 6, an EPUA case having $\zeta_0 = 0.033$, $\Lambda_0 = 0.70$ (several lower- $|\zeta_0|$ EPUA $\Lambda_0 = 0.70$ cases are straining out, as is the UPEA case with the same ζ_0 and Λ_0 ; this will be seen in § 5.1). In these cases, the influence of

the shear enables the second vortex to detrain, and thereby allows for mutual entrainment to occur. It can therefore be said that, in general, the outcome of a given interaction is a function of ζ_0 , Λ_0 , and whether the pair is UPEA or EPUA.

In all cases, the resulting vortex or vortices continue(s) to evolve through viscous diffusion akin to a single vortex under the influence of shear (not shown). In adverse shear, this inevitably leads to filamentation (i.e. detrainment) and, ultimately, breakup. See § 1 and references for general discussion of this case.

4.1. Separation and determination of ζ_{sep}

Shear is seen to cause separation when adverse shear strength surpasses a critical value $\zeta_0 < \zeta_{sep}(\Lambda_0)$, consistent with the analysis in § 2. To determine the value of $\zeta_{sep}(\Lambda_0)$ for a given Λ_0 , a series of simulations is performed for increasing ζ_0 until separation occurs; ζ_{sep} is taken to be the midpoint of the bracketing ζ_0 values. Empirical results for ζ_{sep} are collected in table 1 for a variety of cases, including UPEA, EPUA and UPUA pairs having several Λ_0 values, and both $Re_\Gamma = 5000$ and 1000 (except UPUA cases). Close agreement is seen, across the entire range of parameters considered, between these empirical ζ_{sep} values and predicted $\zeta_{sep,p}$ values computed using (2.18). Although a full exploration of the separation regime is beyond the scope of this study, these results give a general indication of the behaviour of ζ_{sep} for finite-area unequal vortices, and attest to the accuracy of (2.18) within the parameter range considered: ζ_{sep} decreases with decreasing Λ_0 , and is not significantly sensitive to Re_Γ (it is expected that this would remain true as $Re_\Gamma \rightarrow \infty$), or whether the pair is UPEA, EPUA or UPUA. These findings are consistent with previous studies of symmetric pairs in inviscid (Trieling *et al.* 2010) and viscous (Folz & Nomura 2014) flow. Note that (2.18) also predicts dependence on $a_{2,0}/b_0$, which is not considered in this study.

Due to ongoing viscous diffusion, the separated vortices eventually detrain and break up (not shown). There is therefore no distinction between ‘separation without elongation’ and ‘separation with elongation’ in viscous flow, as there is in the inviscid case (Trieling *et al.* 2010). In the cases considered, separation always occurs before filamentation (i.e. detrainment) and breakup: increasing adverse $|\zeta_0|$ simply causes filamentation to begin earlier, and for more disparate pairs (generally, lower Λ_0 , except for the UPUA case) one vortex begins filamentation significantly before the other. It is theoretically possible for a vortex in a UPUA pair to be induced to undergo filamentation and breakup by shear insufficient to cause separation, based on examination of (2.18) in conjunction with known critical values associated with these processes (Moore & Saffman 1971; Mariotti *et al.* 1994; Folz & Nomura 2017; see also this paper’s supplementary material), but these cases are difficult to simulate and are beyond the scope of the present study.

4.2. The vortex-dominated regime

This study focuses on interactions between the two vortices of a pair, which are influenced by the shear. This excludes cases in which the shear causes the vortices to separate, and cases in which the shear essentially forces them together. Separation is precluded when $\zeta_0 > \zeta_{sep}$, as discussed, whereas the latter set of cases is less clearly delineated. However, a reasonable demarcation can be found in the requirement, discussed in § 3, that the vortices be afforded sufficient time to adjust to each other’s presence (i.e. a mutually induced strain field) prior to the onset of detrainment, i.e. that $|\zeta_0| < \zeta_{adj}$. This effectively ensures that the main interaction is initiated primarily through the vortices’ influence (i.e. their intensifying mutual strain).

The vortex-dominated regime, therefore, consists of all cases in the range $\zeta_{sep} < \zeta_0 < \zeta_{adj}$ (since $|\zeta_{adj}| > |\zeta_{sep}|$ for the cases considered in this study). Within this range, all interactions occur primarily between the two vortices, with the shear an external influence. Note that both ζ_{sep} and ζ_{adj} are functions of Λ_0 , and ζ_{adj} depends on $\omega_{1,0}/\omega_{2,0}$ as well (see § 3; in the full parameter space, both are functions of $a_{2,0}/b_0$ as well). The remainder of this study considers only vortex-dominated interactions, unless noted otherwise.

5. Analysis and characterization of vortex-dominated interactions

When two like-signed vortices interact under the influence of external shear, i.e. when the pair's interaction is vortex-dominated, in viscous flow, hendition always occurs. In these cases, the shear affects primarily the occurrence and timing of core detrainment, which can have a significant effect on the ensuing processes and resulting vortex. As seen in § 4, it can even, in some cases, enable entrainment and merger to occur when, in its absence, they would not. In order to examine the shear's net influence on vortex-dominated henditions, their outcomes must be assessed quantitatively. These results can then be related to basic pair parameters, and, ultimately, a general characterization of vortex-dominated henditions developed.

5.1. Quantitative assessment of interaction outcomes in shear

The outcome of any hendition can be assessed quantitatively in terms of an enhancement factor

$$\varepsilon \equiv \frac{\Gamma_{end}}{\Gamma_{2,start}} \quad (5.1)$$

and a corresponding merging efficiency

$$\eta \equiv \frac{\Gamma_{end}}{\Gamma_{tot,start}}, \quad (5.2)$$

based on the ratio of the circulation of the resulting vortex, Γ_{end} , at the end of the main convective interaction, t_{end}^* , to that of the stronger vortex, $\Gamma_{2,start}$, and of the pair combined, $\Gamma_{tot,start}$, respectively, at the start of the main convective interaction, t_{start}^* . (Note that the symbol η has a different meaning here than in § 2.) Mergers correspond to $\varepsilon > 1$, while strainings out correspond to $\varepsilon \approx 1$. Note that η is not a meaningful quantity for strainings out.

In order to identify the appropriate Γ , t_{start}^* and t_{end}^* in the course of the flow development, which proceeds continuously due to the viscosity, a method is used that is similar to that developed for the no-shear case in Folz & Nomura (2017). The vortex cores are identified via a threshold based on the second invariant of the velocity gradient tensor: $II_t^* = II/II_{peak} = 0.10$, where $II = 1/2(\omega^2/2 - S^2)$ is the second invariant at a given location and time, ω is the local vorticity, S is the local strain rate magnitude, and II_{peak} refers to the value of II at the location of the vorticity peak within a contiguous $II > II_t$ region (see Folz & Nomura (2017) for discussion of this choice of II_t^* value).

Aggregate properties of the vortex cores are then computed for the entire flow region meeting the $II > II_t$ criterion, which allows the entire flow development to be monitored

Asymmetric vortex pairs in shear

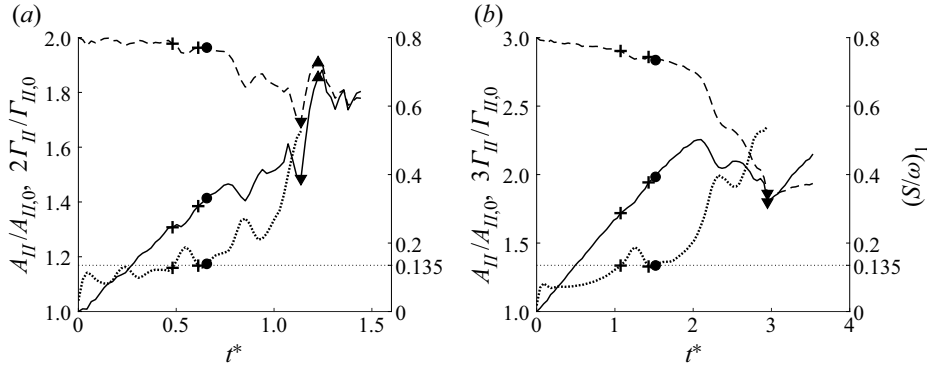


Figure 7. Time development of key quantities for illustrative cases, scaled for better visualization: (a) $\zeta_0 = 0.0167$, $\Lambda_0 = 0.90$; (b) $\zeta_0 = -0.0073$, $\Lambda_0 = 0.70$. Left-hand axis: normalized core area $A_{II}/A_{II,0}$ (solid line); and normalized core circulation $\Gamma_{II}/\Gamma_{II,0}$ (dashed line), scaled by a factor of 2 in (a) and 3 in (b). Right-hand axis: relative straining of weaker vortex $(S/\omega)_1$ (through t^* ; thick dotted line), with critical $(S/\omega)_{cr}$ also indicated (thin horizontal dotted line). The + signs indicate the start and end times of a supercritical peak of $(S/\omega)_{cr}$ and corresponding troughs in $A_{II}/A_{II,0}$ and $\Gamma_{II}/\Gamma_{II,0}$. The \bullet and \blacktriangledown symbols indicate the start and end of core detrainment, t^*_{start} and t^*_{det} , respectively. The \blacktriangle symbols indicate the end of mutual entrainment, t^*_{ent} (occurs in (a) only). See text for definitions of the times.

continuously, including the transition from two vortices to one:

$$A_{II} = \int_{II > II_t} dA \quad (5.3)$$

and

$$\Gamma_{II} = \int_{II > II_t} \omega dA, \quad (5.4)$$

where A_{II} is the aggregate core area, Γ_{II} is the aggregate core circulation, and dA refers to an area element of fluid (similar properties of each individual vortex $i = 1, 2$ are also computed using a separate $II^*_{t,i}$ based on the peak of each, not shown). The time development of the relative straining of each vortex, $(S/\omega)_i$, is also monitored.

The time development of these quantities is presented for the illustrative cases in [figure 7](#); see the supplementary material for the complete flow development of all the cases shown in [figures 3](#) and [4](#). The salient features (which are observed in every case considered) are similar to those observed in the no-shear case (Folz & Nomura 2017). First, there is a period dominated by growth of A_{II} and simultaneous slight decline of Γ_{II} , corresponding to the initial revolving and viscous growth of the pair. This is followed by diminishing growth (until a local maximum is reached) then decline of A_{II} and simultaneous more rapid decline of Γ_{II} , until each reaches a local minimum, corresponding to core detrainment. In some cases (such as that in [figure 7a](#)), these local minima are followed by rapid rises to local maxima, i.e. spikes, corresponding to mutual entrainment.

The most significant effect of shear is the introduction of additional local minima in the Γ_{II} development (with corresponding variations in the A_{II} development, e.g. beginning at $t^* = 0.50$ in [figure 7\(a\)](#), and at $t^* = 1.1$ in [figure 7\(b\)](#)). It is seen that these ‘troughs’ correspond to local maxima, or ‘bumps’, in the time development of $(S/\omega)_1$ (which exhibits net growth due to viscous diffusion intensifying $(S/\omega)_1$), which in turn correspond to the periodic amplified deformation, associated with the vortices’ orientation, observed in [§ 4](#). (The squares and diamonds in [figure 5](#) correspond to the peaks of bumps in $(S/\omega)_1$

in [figure 7](#); corresponding bumps also occur in $(S/\omega)_2$, not shown here.) Notably, $(S/\omega)_i$ of either vortex may temporarily exceed the critical $(S/\omega)_{cr} = 0.135$ (associated with core detrainment) one or more times, with negligible evident detrainment, before $(S/\omega)_1$ (and in some cases, $(S/\omega)_2$) ultimately surpasses it terminally as A_{II} growth diminishes and Γ_{II} decline accelerates.

Due to these nonlinearities, t_{start}^* is taken to be the earlier time at which one vortex achieves – and thereafter maintains – $(S/\omega)_i > (S/\omega)_{cr} = 0.135$ through to the end of detrainment. (In the no-shear case, t_{start}^* had been identified as the time of deviation of A_{II} from linear growth – see [Folz & Nomura \(2017\)](#); t_{start}^* as identified in the present manner produces similar results in those cases, not shown.) This time is indicated for the illustrative cases in [figure 7](#) (in [figures 3\(b–e\)](#) and [4\(a–f\)](#), column 4 corresponds to t_{start}^*). Maintaining the critical $(S/\omega)_{cr} = 0.135$ value has been seen to correspond to detrainment both here and in the no-shear case, and is also consistent with the value observed in simulations of a single Gaussian vortex in adverse shear (e.g. [Mariotti *et al.* 1994](#)), suggesting that this is a general critical value for Gaussian vortices subject to external strain. In this study, the first detraining vortex is always vortex 1. This identification of t_{start}^* with the maintaining of $(S/\omega)_1 > (S/\omega)_{cr}$ is consistent with the observation in [Trieling *et al.* \(2010\)](#) that symmetric pairs in shear always merge when their peak–peak distance remains within the critical merging criterion for symmetric pairs without shear; it is noted, though, that they do observe merger to occur in cases (typically having favourable shear) in which the vortices only temporarily surpass the critical criterion. The choice of t_{start}^* here therefore likely constitutes a conservative estimate for the start of the main convective interaction.

The end of the interaction, t_{end}^* , is taken to be the time of the first peak (i.e. spike) immediately following the minimum if there is one (i.e. the end of entrainment, t_{ent}^*), or the time of the local minimum otherwise (i.e. the end of detrainment, t_{det}^*). These times are indicated for the illustrative cases in [figure 7](#) (and in [figures 3\(b–e\)](#) and [4\(a–f\)](#), column 5 corresponds to t_{det}^* , and column 6 to t_{ent}^*). In all cases considered, t_{end}^* corresponds to the existence of only a single vortical structure meeting the $II > II_I$ criterion. These are identical to the criteria used in the no-shear case ([Folz & Nomura 2017](#)).

5.2. The influence of shear on the timing and duration of detrainment

The shear has a significant influence on the timing of detrainment, as seen in [figures 8\(a,b\)](#), which show t_{start}^* and $\Delta_d t^* = t_{det}^* - t_{start}^*$, the duration of the detrainment-dominated portion of the main convective interaction, respectively. The large degree of variation of t_{start}^* with ζ_0 reflects the influence of shear on b , and thereby the overall growth of $(S/\omega)_i$ leading to detrainment: lowering and increasing t_{start}^* , i.e. accelerating or delaying the onset of detrainment, derives from shear reducing or increasing b from b_0 , respectively (here associated with favourable and adverse shear; this is discussed further below). The variation of t_{start}^* with Λ_0 (and whether the pair is UPEA or EPUA) is consistent with that observed in the no-shear case: t_{start}^* decreases for increasing pair disparity (lower Λ_0 ; [Folz & Nomura 2017](#)). It is also noted that as ζ_0 increases from 0, the variation of t_{start}^* with Λ_0 is reduced, consistent with the (increasingly strong, favourable) shear playing an increasingly significant role in the initiation of detrainment. The observed variation of $\Delta_d t^*$ likewise reflects the influence of shear on b , with reduction and increase likewise generally shortening and prolonging the duration of detrainment, although the effect here is not strictly monotonic. This is attributed to the complexity of the detrainment process,

Asymmetric vortex pairs in shear

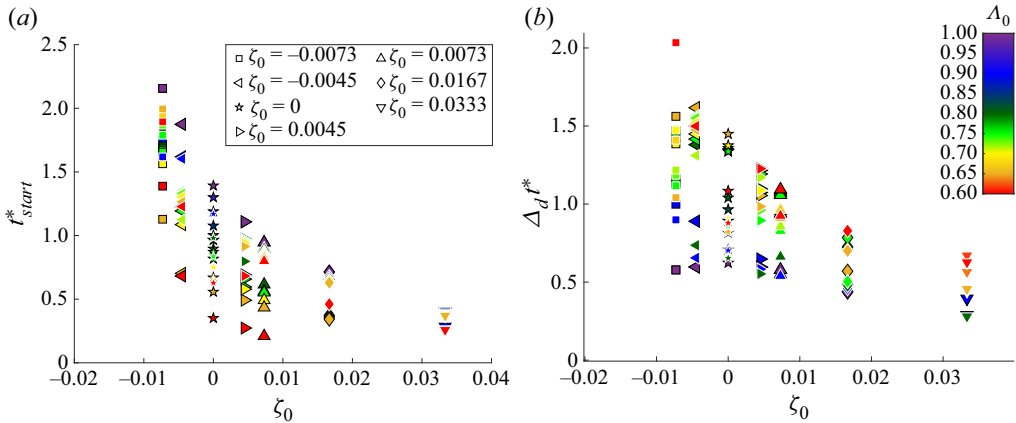


Figure 8. For vortex-dominated henditions: (a) time of interaction start, t_{start}^* , and (b) the duration of detrainment, $\Delta_d t^* \equiv t_{det}^* - t_{start}^*$, as functions of ζ_0 and Λ_0 (both UPEA and EPUA). The meanings of symbol shapes and colours are indicated in (a,b), respectively; a black outline indicates UPEA cases (and symmetric), and a white outline indicates EPUA cases ($Re_\Gamma = 5000$).

as well as the method of assigning t_{start}^* and t_{end}^* . It is also seen that $\Delta_d t^*$ increases with decreasing Λ_0 (consistent with Folz & Nomura 2017), and that in some cases this can be quite significant, especially for $\zeta_0 < 0$.

It should be understood that the net influence of the shear on $\Delta_d t^*$ derives not only from the time variation of b , but also from directional effects that inhibit core detrainment. In order to examine this influence, the angle ϕ_i is computed for each vortex $i = 1, 2$, where ϕ_i is the angle between the peak–peak axis and $e_{pk,i}$, the unit vector corresponding to the direction of principal extensional strain evaluated at the vorticity peak. The angle ϕ_i serves as an instantaneous indicator of the vortex’s response to the net directional influence of the strain rate fields induced by the shear and the other vortex as their relative prevalence and direction vary in time. The time variations of $\cos^2(\phi_i)$ for each vortex for no-shear cases having $\Lambda_0 = 0.90$ and $\Lambda_0 = 0.70$ are presented in figures 9(a,b), and it is seen that $\cos^2(\phi_i) \approx 0.5$ is maintained (i.e. $\phi_i \approx 45^\circ$, after the initial adjustment period) until detrainment begins, after which $\cos^2(\phi_i)$ decreases (i.e. ϕ_i increases); this occurs for both vortices in the $\Lambda_0 = 0.90$ case – a merger – and only for the weaker vortex in the $\Lambda_0 = 0.70$ case – a straining out. It can therefore be said that $\cos^2(\phi_i) < 0.5$ is associated with core detrainment. When shear is present (shown for the illustrative cases in figures 9c,d), its principal extensional strain rate remains fixed in the Eulerian frame (oriented 45° from the background flow direction), which initially causes $\cos^2(\phi_i)$ of both vortices to oscillate about 0.5 as they revolve; this occurs such that the bumps in $(S/\omega)_i$ correspond to maximum $\cos^2(\phi_i)$, i.e. when the directional effects are unfavourable for detrainment. This may explain why little evident detrainment occurs even when $(S/\omega)_i > (S/\omega)_{cr}$ during a bump. After t_{start}^* , one vortex (at least) maintains $(S/\omega)_i > (S/\omega)_{cr}$ and $\cos^2(\phi_i) < 0.5$ simultaneously, thereby undergoing detrainment and causing hendition to occur. These observations suggest that in order for core detrainment to occur, the vortex must maintain both sufficient relative straining ($(S/\omega)_i > (S/\omega)_{cr}$) and conducive directionality ($\cos^2(\phi_i) < 0.5$) of its straining response.

It is critical to note that accelerating/delaying t_{start}^* and shortening/prolonging $\Delta_d t^*$ are not necessarily associated with ‘favourable’ or ‘adverse’ shear. If the vortices are initially oriented along the shear direction, then the favourable shear delays/prolongs while adverse

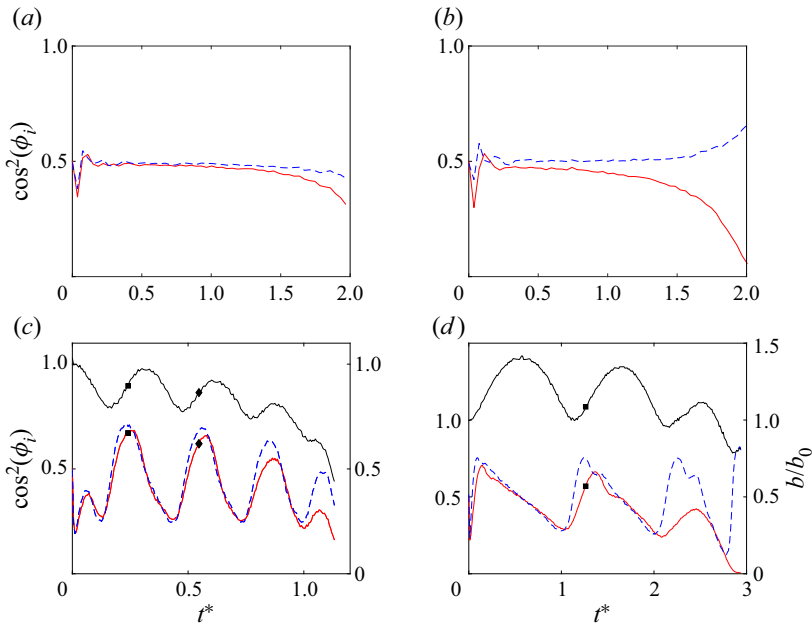


Figure 9. Time development of $\cos^2(\phi_i)$, where ϕ_i is the angle between the peak–peak axis and the principal extensional strain eigenvector at each peak, $e_{pk,i}$ (left-hand axis; solid red line shows vortex 1, dashed blue line shows vortex 2), for no-shear cases having (a) $\Lambda_0 = 0.90$ and (b) $\Lambda_0 = 0.70$; and the illustrative shear UPEA cases having (c) $\zeta_0 = 0.0167$, $\Lambda_0 = 0.90$ and (d) $\zeta_0 = -0.0073$, $\Lambda_0 = 0.70$. In all cases, $Re_\Gamma = 5000$. In (c,d), the time development of b/b_0 is also included for reference (right-hand axis; solid black line), and \blacksquare (and \blacklozenge) indicate times of first (and, in (c), second) local S/ω peak (see figures 5 and 7).

shear accelerates/shortens (since, in this orientation, the vortices are initially located at minimum b in the favourable case and maximum b in the adverse). This can be seen in table 2, which shows t_{start}^* and $\Delta_d t^*$ for equivalent cases having each initial orientation (i.e. maintaining all pair parameters described in § 3). A full exploration of the relationship between the initial orientation, the flow development, and outcomes is beyond the scope of this study, but it can be concluded that the observed effects of shear on timing derive primarily from the relative motion of the vortices that it engenders, and not, strictly speaking, the shear’s relative sense.

5.3. Results for ε and η

It has been seen that shear affects the timing and duration of core detrainment, and it is known that the outcome of an asymmetric pair interaction derives from the relative timing of detrainment and destruction of the vortices (Brandt & Nomura 2010). The influence of the shear on interaction outcomes is therefore most significant when the outcome of the case is particularly sensitive to changes in this timing. To examine this, and the influence of shear on interaction outcomes overall, ε and η are computed for every case using (5.1) and (5.2).

Figure 10 shows each henthion case, with ε indicated via colour, for both UPEA and EPUA cases (similar trends are observed for η). Linear interpolation has also been employed to estimate ε values between the simulated cases, in order to better visualize the overall trends. In the broadest sense, the variation of ε is similar to that of the

ζ_0	Λ_0	Horiz t_{start}^*	Vert t_{start}^*	Horiz Δt^*	Vert Δt^*	Horiz ε	Vert ε
0.0073	1.0	0.95	1.79	0.58	0.58	2.19	1.96
0.0073	0.9	0.90	1.50	0.55	1.10	1.81	1.81
0.0073	0.7	0.49	0.98	0.94	1.43	1.02	1.04
-0.0073	1.0	2.16	1.05	0.58	0.42	2.09	2.09
-0.0073	0.9	1.75	0.75	1.00	0.90	1.81	1.78
-0.0073	0.7	1.56	0.27	1.39	1.07	1.01	1.00
0.0167	1.0	0.71	2.07	0.44	0.55	1.94	2.05
0.0167	0.9	0.66	1.84	0.43	0.79	1.80	1.81
0.0167	0.7	0.35	1.37	0.70	1.33	1.03	1.06

Table 2. Time of start of core detrainment, t_{start}^* , and duration of detrainment, $\Delta t^* \equiv t_{det}^* - t_{start}^*$, for equivalent UPEA cases initially oriented horizontally (Horiz) and vertically (Vert) ($Re_\Gamma = 5000$).

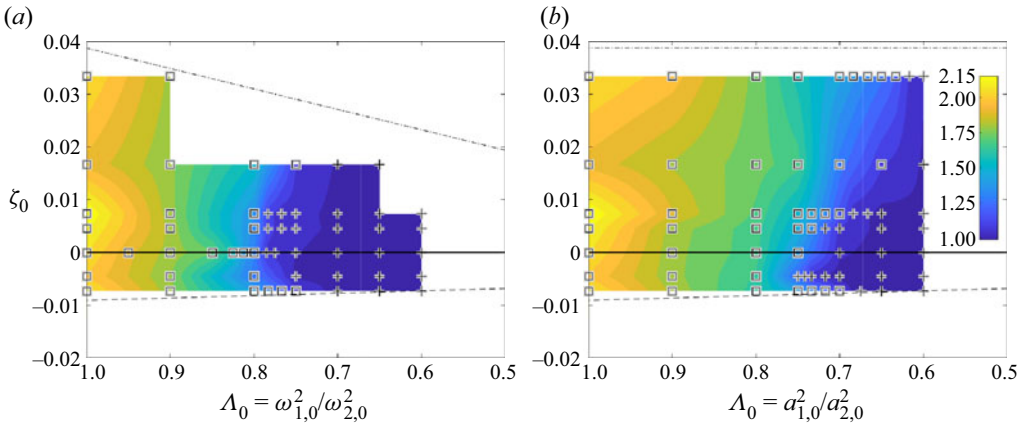


Figure 10. Interaction outcomes for vortex-dominated henditions for (a) UPEA and (b) EPUA cases. Symbols indicate the outcomes of the cases included in figure 8, categorized: \square indicates merger; $+$ indicates straining out (see § 5.1). Colours indicate enhancement factor ε : values for each denoted case are exact, while those in between are produced by linear interpolation (both plots use same colour map, indicated in (b)). The solid black line indicates $\zeta_0 = 0$, the dashed line indicates $\zeta_{sep,p}$ (see § 2), and the dash-dotted line indicates ζ_{adj} (see §§ 3 and 4). The data for the no-shear ($\zeta_0 = 0$) cases were presented previously in Folz & Nomura (2017). Note that ε inherently declines with decreasing Λ_0 , since the theoretical maximum is $\varepsilon_{max} = 1 + \Lambda_0$. In all cases, $Re_\Gamma = 5000$.

no-shear case: ε is maximal ($\varepsilon \approx 2$) for symmetric pairs, and minimal ($\varepsilon \approx 1$) for highly disparate ones (approximately $\Lambda_0 < 0.70$ for UPEA, and $\Lambda_0 < 0.60$ for EPUA). The $\Lambda_{0,cr}$ value at which this minimum ε is reached is seen to vary with ζ_0 , particularly in the transitional range (approximately $0.80 \geq \Lambda_0 \geq 0.70$ for UPEA, and $0.80 \geq \Lambda_0 \geq 0.60$ for EPUA), being generally lower for higher $|\zeta_0|$ (with the notable exception of the $\zeta_0 \leq 0$, $0.75 \geq \Lambda_0 \geq 0.70$ subregion). More generally, the variation of ε with ζ_0 is not always monotonic, for $\Lambda_0 > \Lambda_{0,cr}$.

Also indicated in figure 10, via the symbols, is the occurrence of mutual entrainment (i.e. merger) or not (i.e. straining out) in each case (as ascertained from the presence of one or more spikes post- t_{det}^* in the Γ_{II} time development; see § 5.1). It is seen that the presence of shear can engender entrainment in some cases where it does not occur in the equivalent no-shear case, and that this typically occurs for more disparate pairs when shear is stronger

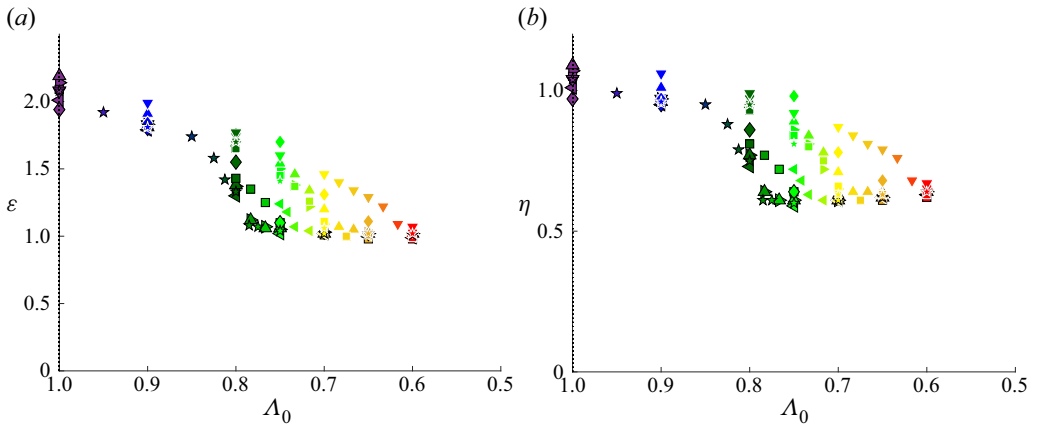


Figure 11. For vortex-dominated henditions: (a) ε and (b) η , as functions of Λ_0 . See figure 8 for meanings of symbol shapes, colours and outlines. In all cases, $Re_T = 5000$.

(again there are notable exceptions, particularly in the EPUA $\zeta_0 \leq 0$, $0.75 \geq \Lambda_0 \geq 0.70$ subregion). This promotion of merger is attributed to the shear – of either sense – altering the rate of increase of $(S/\omega)_i$ of each vortex, making detrainment of the second vortex more likely prior to the destruction of the first.

The variations of ε and η with ζ_0 and Λ_0 for all hendition cases are presented in figure 11. It is seen that, within the transition region, cases with $\zeta_0 \neq 0$ typically have higher ε and η than the no-shear case with the same Λ_0 , and that increasingly favourable shear generally (though not universally) results in greater enhancement and more efficient merger for EPUA cases. (Note that the variation for the symmetric case results largely from the use of II_t in conjunction with its uniquely reciprocal mutual strain.) The handful of cases with lower ε and η than in the no-shear case have $\zeta_0 < 0$: the weaker $\zeta_0 = -0.0045$ cases always produce $\varepsilon < \varepsilon(\zeta_0 = 0)$ for a given Λ_0 , while the stronger $\zeta_0 = -0.0073$ begins to produce $\varepsilon > \varepsilon(\zeta_0 = 0)$ for more disparate pairs ($\Lambda_0 \leq 0.75$ for EPUA) only until the straining out regime is reached, i.e. stronger adverse shear better enables entrainment to occur. Similar trends are observed in the $\varepsilon - \Lambda$ and $\eta - \Lambda$ variations, where Λ is evaluated at t_{start}^* (not shown). It is noted that the initially vertical cases considered in § 5.2 produce ε and η similar to those for their initially horizontal counterparts (table 2; not otherwise included in the present results or discussion).

An example of shear of either sense promoting merger is presented in figures 12(a,b,c), which show the time development of $(S/\omega)_i$ for EPUA $\Lambda_0 = 0.70$ cases having $\zeta_0 = 0.033$, no shear and $\zeta_0 = -0.0073$, respectively. In these cases, entrainment does not occur for the no-shear case, but it does occur for $\zeta_0 = 0.033$ ($\varepsilon = 1.46$; vorticity contours for this case are shown in figure 6), and to a small degree for $\zeta = -0.0073$ ($\varepsilon = 1.11$; vorticity contours not shown). It is seen that the influence of the shear causes $(S/\omega)_2$ to surpass $(S/\omega)_{cr}$ in both $\zeta_0 \neq 0$ cases, allowing detrainment of the second vortex to occur. For the $\zeta_0 = 0.033$ case, this is done primarily by accelerating the rate of increase of $(S/\omega)_2$ (i.e. reducing t_{start}^*); for the $\zeta = -0.0073$ case, this is done primarily by prolonging the detrainment of vortex 1 (i.e. increasing Δdt^*), allowing $(S/\omega)_2$ to increase sufficiently to surpass $(S/\omega)_{cr}$ prior to the end of the interaction.

Asymmetric vortex pairs in shear

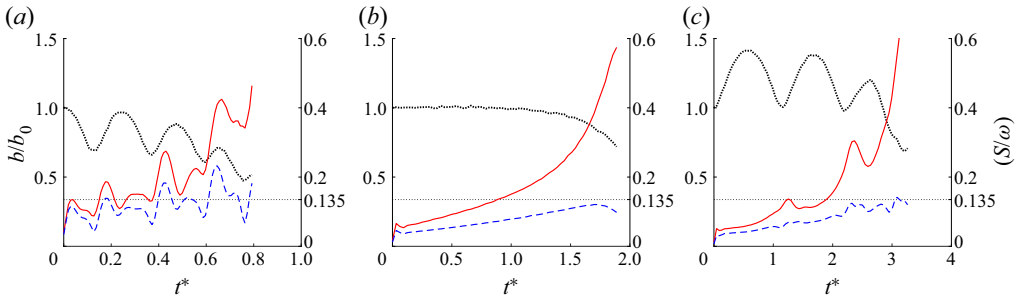


Figure 12. Time development of $(S/\omega)_1$ and $(S/\omega)_2$ (red solid and blue dashed lines, respectively; right-hand axis), along with b/b_0 (thick dotted line; left-hand axis), for EPUA cases having $Re_\Gamma = 5000$ and $\Lambda_0 = 0.70$, with (a) $\zeta_0 = 0.0167$, (b) $\zeta_0 = 0$ (no shear), and (c) $\zeta_0 = -0.0073$. In all plots, the horizontal thin dotted line indicates $(S/\omega)_{cr} = 0.135$. The $\zeta_0 \neq 0$ cases are mergers ($\varepsilon > 1$), whereas the no-shear case is a straining out ($\varepsilon \approx 1$).

5.3.1. Mutuality and the fundamental characterization of hendidions in shear

Fundamentally, the outcome of the interaction of two like-signed vortices derives from the degree of mutuality of the interaction. In the no-shear case, Folz & Nomura (2017) introduced a mutuality parameter $MP = (S/\omega)_1/(S/\omega)_2$, which compares the relative straining of each vortex at t_{start}^* , and thereby captures the degree of mutuality of the interaction. When the relative straining of both vortices is similar at t_{start}^* (approximately $1 \leq MP < 1.8$ for $Re_\Gamma = 5000$), the second vortex can begin to detrain before the first is destroyed, enabling mutual entrainment (i.e. merger occurs); when the disparity is greater (approximately $MP > 1.8$), it cannot, and the first detrainng vortex is simply destroyed (i.e. straining out occurs). In the vortex-dominated regime, MP is computed for the shear cases in the same manner.

Figure 13 shows the variations of ε and η with MP . A generally monotonic relationship is observed between ε and MP (likewise η and MP), with $\varepsilon \approx 2$ (and $\eta \approx 1$) near $MP = 1$, then generally declining as MP increases until $MP \approx 2$, at which point $\varepsilon \approx 1$ is reached and thereafter maintained (recall that η ceases to be a meaningful quantity for strainings out). However, significantly more scatter is observed in the shear case (as compared with figure 9 in Folz & Nomura 2017). This is attributed to MP being a pointwise quantity, and therefore sensitive to significant and rapid variations as the vortices revolve.

However, MP is related closely to the vortex enstrophy ratio, an integrated quantity less susceptible to fluctuations:

$$\frac{Z_2}{Z_1} = \frac{\int_{\Pi > \Pi_{t,2}} \omega_2^2 dA_2}{\int_{\Pi > \Pi_{t,1}} \omega_1^2 dA_1}, \quad (5.5)$$

where the integral is evaluated for each vortex at t_{start}^* . This quantity was also seen to effectively characterize the variation of ε and η in the no-shear case (Folz & Nomura 2017).

Figure 14 shows the variations of ε and η with Z_2/Z_1 . It is seen that the scatter is greatly reduced (even for high $|\zeta_0|$), such that the variation is essentially monotonic outside of a transition region, reached at 1.65 ± 0.01 and extending to 1.91 ± 0.02 (where the margins of error for each are found from the extremal midpoint between a merger and a straining out case). In this region, cases having similar Z_2/Z_1 but different ζ_0 ,

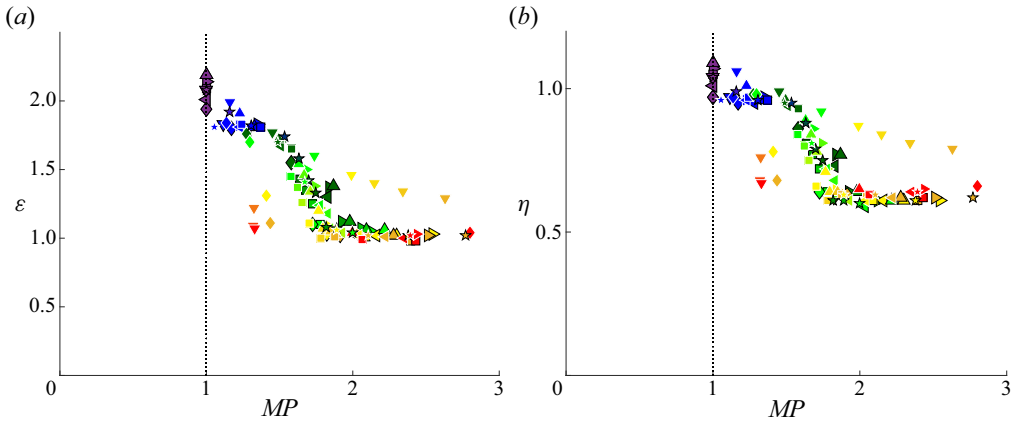


Figure 13. For vortex-dominated henditions: (a) ε and (b) η as functions of $MP = (S/\omega)_1/(S/\omega)_2$. See figure 8 for meanings of symbol shapes, colours and outlines. The dotted line indicates $MP = 1$. In all cases, $Re_\Gamma = 5000$.

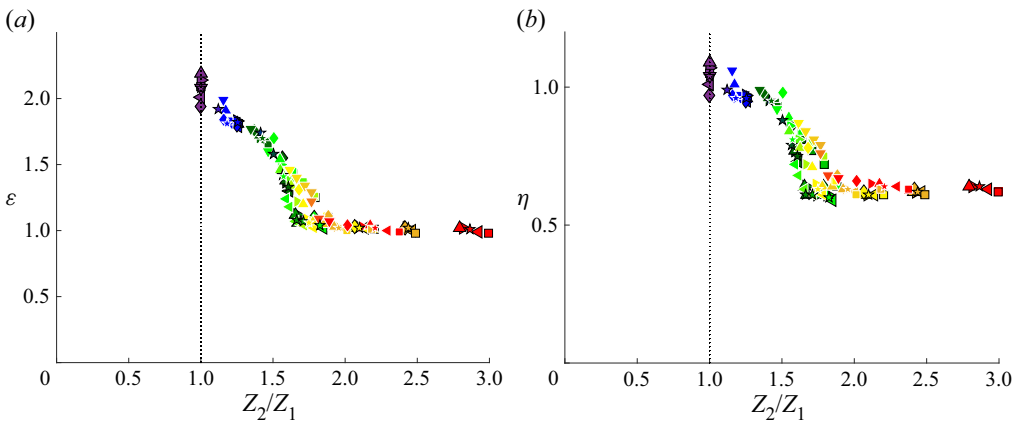


Figure 14. For vortex-dominated henditions: (a) ε and (b) η as functions of Z_2/Z_1 . See figure 8 for meanings of symbol shapes, colours and outlines. The dotted line indicates $Z_2/Z_1 = 1$. In all cases, $Re_\Gamma = 5000$.

Λ_0 and/or UPEA/EPUA status can produce significantly different ε and η , with higher $|\zeta_0|$ generally (though not universally) corresponding to higher ε and η . The consistently lesser enhancement and less efficient merging when weak adverse shear is present ($\zeta_0 = -0.0045$) are attributed to greater dissipation of detrained fluid due to the increase of b , while the greater enhancement and more efficient merging produced by stronger adverse shear ($\zeta_0 = -0.0073$) are attributed to the interaction being sufficiently prolonged to enable entrainment. The lower bound of the transition region is comparable to the critical $(Z_2/Z_1)_{cr} \approx 1.63 \pm 0.03$ for straining out observed in the no-shear case, and merger cases having greater Z_2/Z_1 correspond to higher $|\zeta_0|$.

As such, it can be concluded that favourable and sufficiently strong adverse shear (approximately $\zeta_0 < -0.0045$) promote enhancement and merger for interactions that are moderately disparate (i.e. having approximately $1.65 < Z_2/Z_1 < 1.9$). Efficient merger occurs in interactions with a high degree of mutuality, regardless of shear strength

(typically $\eta > 0.85$ for $Z_2/Z_1 < 1.65$), while more disparate ones always result in straining out of the weaker vortex ($\varepsilon \approx 1$ for $Z_2/Z_1 > 1.9$).

The fact that the variations of ε and η with Z_2/Z_1 are generally monotonic is taken as evidence that the choice of t_{start}^* ($(S/\omega)_1 > (S/\omega)_{cr} = 0.135$ terminally) does effectively characterize the start of convective detrainment (see § 5.2). These trends are also observed when only the relative vorticity is considered (not shown), indicating that they reflect the shear's effect on the physical mechanisms of vortex interaction and not spurious consequences of the use of II_t .

6. Summary and discussion

This study considers the interaction of a pair of unequal vortices in background shear with finite viscosity. In these cases, the flow development is determined by the relative significance of the vortices' mutual influence and that of the shear. Sufficiently adverse shear causes the vortices to separate; the critical adverse shear strength for separation, ζ_{sep} , varies with the pair's circulation ratio Λ_0 (and aspect ratio), and its empirical values are well-predicted by point-vortex analysis. Otherwise, the interaction between the vortices is a hendition (§ 1.1), resulting in a single vortex.

In henditions occurring in background shear, the flow development is essentially governed by three constituent external influences occurring simultaneously, whose relative significance varies in time: the shear causes the peak–peak distance b between the vortices to vary as they revolve; the vortices influence each other through their mutually induced strain, which depends on b ; and the strain induced by the constant shear acts directly on each vortex. When the shear is strongly favourable, it causes such significant reduction of b and amplified deformation of the vortices that it is the principal cause of hendition; otherwise, when the shear is weakly favourable or weakly adverse, the flow is vortex-dominated.

In vortex-dominated henditions in shear, viscous diffusion causes the vortices' mutually induced strain to become predominant, which enables sufficient persistence of straining for one vortex to begin detraining core fluid: the relative straining remains sufficiently strong in magnitude ($(S/\omega)_i > (S/\omega)_{cr} = 0.135$ for detraining vortex i), and the directionality of the vortex's response to the external strain field maintains a conducive relative orientation ($\cos^2(\phi_i) < 0.5$) for sustained detrainment despite the continuing influence of shear on b and on each vortex directly. The flow development then proceeds similarly to the no-shear case: if the second vortex is induced to detrain before the first is destroyed, then a two-way interaction leads to a mutual entrainment process that produces an enhanced resulting vortex i.e. merger occurs; otherwise, the interaction is essentially one-way and the detraining vortex is broken up, leaving the other largely unaffected, i.e. straining out occurs.

The post-interaction vortex is assessed quantitatively in terms of an enhancement factor ε and a merging efficiency η , using a method adapted from one utilized in the no-shear case (Folz & Nomura 2017). It is found that all vortex-dominated hendition outcomes across the parameter range considered are effectively characterized by the pair's core enstrophy ratio at the start of detrainment, Z_2/Z_1 , which encapsulates the mutuality of the interaction similarly to $MP = (S/\omega)_1/(S/\omega)_2$ (utilized previously in the no-shear case) but is less sensitive to the time variation caused by the shear. For Z_2/Z_1 near unity, merger essentially conserves circulation, while mergers between more disparate vortices become less efficient until straining out occurs. Within the transition region, approximately $1.65 < Z_2/Z_1 < 1.9$, weak adverse shear reduces enhancement; otherwise, the presence of

shear of either sense generally promotes enhancement and merger relative to the no-shear case (in which straining out occurs for $Z_2/Z_1 > (Z_2/Z_1)_{cr} \approx 1.63$ for $Re_\Gamma = 5000$, similar to the value at which it first occurs with shear present). In favourable shear, this results from more rapid increase of $(S/\omega)_2$ due to reduction of b , while in adverse shear, this results from prolonging the interaction due to a combination of increase of b and periodic detrainment-inhibiting orientation effects allowing $(S/\omega)_2$ to reach $(S/\omega)_{cr}$ (with simultaneous $\cos^2(\phi_i) < 0.5$) before the first vortex is destroyed.

Additional study must examine vortex pair parameters beyond those considered here. In particular, it is possible that the boundary values of the Z_2/Z_1 transition region may vary with parameters such as the Reynolds number or initial aspect ratio, either of which would be expected to affect the rate of increase of $(S/\omega)_i$ and therefore promote or inhibit detrainment of the second vortex. It has also been seen that the initial orientation of the vortices relative to the shear is significant: certain effects can be associated with the opposite sense of shear in the orthogonal initial orientation (e.g. when the vortices are initially oriented along the shear direction, favourable shear increases b and prolongs the interaction, while adverse shear reduces and shortens). Moreover, it would be desirable to consider a time-varying background flow, which might better reflect that experienced by a vortex pair in turbulence (the concept of persistence of straining leading to detrainment may be a particularly significant concept in such flows). It is hoped that the current study may provide a step towards a more all-encompassing characterization of vortex interactions in background flow that incorporates these additional parameters, and others (the influence of an opposite-signed vortex would be another priority for consideration). Such studies remain for future work.

Supplementary material. Supplementary material and movies are available at <https://doi.org/10.1017/jfm.2023.525>.

Funding. This research received no specific grant from any funding agency, commercial or not-for-profit sectors.

Declaration of interests. The authors report no conflict of interest.

Author ORCIDs.

Patrick J.R. Folz <https://orcid.org/0000-0001-8441-411X>;

Keiko K. Nomura <https://orcid.org/0000-0003-3872-2722>.

REFERENCES

- BAGGALEY, A.W. & BARENGHI, C.F. 2018 Decay of homogeneous two-dimensional quantum turbulence. *Phys. Rev. A* **97** (3), 033601.
- BRANDT, L.K. & NOMURA, K.K. 2006 The physics of vortex merger: further insight. *Phys. Fluids* **18** (5), 051701.
- BRANDT, L.K. & NOMURA, K.K. 2007 The physics of vortex merger and the effects of ambient stable stratification. *J. Fluid Mech.* **592**, 413–446.
- BRANDT, L.K. & NOMURA, K.K. 2010 Characterization of the interactions of two unequal co-rotating vortices. *J. Fluid Mech.* **646**, 233–253.
- BURGESS, B.H., DRITSCHEL, D.G. & SCOTT, R.K. 2017*a* Extended scale invariance in the vortices of freely evolving two-dimensional turbulence. *Phys. Rev. Fluids* **2** (11), 114702.
- BURGESS, B.H., DRITSCHEL, D.G. & SCOTT, R.K. 2017*b* Vortex scaling ranges in two-dimensional turbulence. *Phys. Fluids* **29** (11), 111104.
- CARTON, X., MAZE, G. & LEGRAS, B. 2002 A two-dimensional vortex merger in an external strain field. *J. Turbul.* **3**, N45.
- CERRETELLI, C. & WILLIAMSON, C.H.K. 2003 The physical mechanism for vortex merging. *J. Fluid Mech.* **475**, 41–77.

Asymmetric vortex pairs in shear

- DRITSCHEL, D.G. & WAUGH, D.W. 1992 Quantification of the inelastic interaction of unequal vortices in two-dimensional vortex dynamics. *Phys. Fluids A* **4** (8), 1737–1744.
- FOLZ, P.J.R. & NOMURA, K.K. 2014 Interaction of two equal co-rotating viscous vortices in the presence of background shear. *Fluid Dyn. Res.* **46** (3), 031423.
- FOLZ, P.J.R. & NOMURA, K.K. 2017 A quantitative assessment of viscous asymmetric vortex pair interactions. *J. Fluid Mech.* **829**, 1–30.
- FU, W., LI, H., LUBOW, S., LI, S. & LIANG, E. 2014 Effects of dust feedback on vortices in protoplanetary disks. *Astrophys. J. Lett.* **795** (2), L39.
- GERZ, T., SCHUMANN, U. & ELGHOBASHI, S.E. 1989 Direct numerical simulation of stratified homogeneous turbulent shear flows. *J. Fluid Mech.* **200**, 563–594.
- HUANG, M.J. 2005 The physical mechanism of symmetric vortex merger: a new viewpoint. *Phys. Fluids* **17** (7), 074105.
- HUANG, M.J. 2006 A comparison between asymmetric and symmetric vortex mergers. *WSEAS Trans. Fluid Mech.* **1** (5), 488–496.
- HURST, N.C., DANIELSON, J.R., DUBIN, D.H.E. & SURKO, C.M. 2016 Evolution of a vortex in a strain flow. *Phys. Rev. Lett.* **117** (23), 235001.
- JING, F., KANSO, E. & NEWTON, P.K. 2012 Insights into symmetric and asymmetric vortex mergers using the core growth model. *Phys. Fluids* **24** (7), 073101.
- KIMURA, Y. & HASIMOTO, H. 1985 Motion of two identical point vortices in a simple shear flow. *J. Phys. Soc. Japan* **54** (11), 4069–4072.
- KIMURA, Y. & HERRING, J.R. 2001 Gradient enhancement and filament ejection for a non-uniform elliptic vortex in two-dimensional turbulence. *J. Fluid Mech.* **439**, 43–56.
- LE DIZÈS, S. & LAPORTE, F. 2002 Theoretical predictions for the elliptical instability in a two-vortex flow. *J. Fluid Mech.* **471**, 169–201.
- LE DIZÈS, S. & VERGA, A. 2002 Viscous interactions of two co-rotating vortices before merging. *J. Fluid Mech.* **467**, 389–410.
- LEGRAS, B. & DRITSCHEL, D.G. 1993 Vortex stripping and the generation of high vorticity gradients in two-dimensional flows. In *Advances in Turbulence IV* (ed. F.T.M. Nieuwstadt), pp. 445–455. Springer.
- LEGRAS, B., DRITSCHEL, D.G. & CAILLOL, P. 2001 The erosion of a distributed two-dimensional vortex in a background straining flow. *J. Fluid Mech.* **441**, 369–398.
- LEWEKE, T., LE DIZÈS, S. & WILLIAMSON, C.H.K. 2016 Dynamics and instabilities of vortex pairs. *Annu. Rev. Fluid Mech.* **48**, 507–541.
- MARIOTTI, A., LEGRAS, B. & DRITSCHEL, D.G. 1994 Vortex stripping and the erosion of coherent structures in two-dimensional flows. *Phys. Fluids* **6** (12), 3954–3962.
- MARQUES ROSAS FERNANDES, V.H., KAMP, L.P.J., VAN HEIJST, G.J.F. & CLERCX, H.J.H. 2016 Interaction of monopoles, dipoles, and turbulence with a shear flow. *Phys. Fluids* **28** (9), 093603.
- MAZE, G., CARTON, X. & LAPEYRE, G. 2004 Dynamics of a 2D vortex doublet under external deformation. *Regular Chaotic Dyn.* **9** (4), 477–497.
- MELANDER, M.V., ZABUSKY, N.J. & MCWILLIAMS, J.C. 1987 Asymmetric vortex merger in two dimensions: which vortex is ‘victorious’? *Phys. Fluids* **30** (9), 2610–2612.
- MELANDER, M.V., ZABUSKY, N.J. & MCWILLIAMS, J.C. 1988 Symmetric vortex merger in two dimensions: causes and conditions. *J. Fluid Mech.* **195**, 303–340.
- MEUNIER, P., EHRENSTEIN, U., LEWEKE, T. & ROSSI, M. 2002 A merging criterion for two-dimensional co-rotating vortices. *Phys. Fluids* **14** (8), 2757–2766.
- MEUNIER, P., LE DIZÈS, S. & LEWEKE, T. 2005 Physics of vortex merging. *C. R. Phys.* **6** (4–5), 431–450.
- MOORE, D.W. & SAFFMAN, P.G. 1971 Structure of a line vortex in an imposed strain. In *Aircraft Wake Turbulence and its Detection* (ed. J.H. Olsen, A. Goldberg & M. Rogers), pp. 339–354. Springer.
- PAIREAU, O., TABELING, P. & LEGRAS, B. 1997 A vortex subjected to a shear: an experimental study. *J. Fluid Mech.* **351**, 1–16.
- PERRON, X. & CARTON, X. 2010 2D vortex interaction in a non-uniform flow. *Theor. Comput. Fluid Dyn.* **24** (1–4), 95–100.
- RYZHOV, E.A., KOSHEL, K.V. & CARTON, X. 2012 Passive scalar advection in the vicinity of two point vortices in a deformation flow. *Eur. J. Mech. (B/Fluids)* **34**, 121–130.
- SUTYRIN, G.G. 2019 On vortex intensification due to stretching out of weak satellites. *Phys. Fluids* **31** (7), 075103.
- TABELING, P. 2002 Two-dimensional turbulence: a physicist approach. *Phys. Rep.* **362** (1), 1–62.
- TRIELING, R.R., DAM, C.E.C. & VAN HEIJST, G.J.F. 2010 Dynamics of two identical vortices in linear shear. *Phys. Fluids* **22** (11), 117104.

- TRIELING, R.R., VELASCO FUENTES, O.U. & VAN HEIJST, G.J.F. 2005 Interaction of two unequal corotating vortices. *Phys. Fluids* **17** (8), 087103.
- VELASCO FUENTES, O.U. 2005 Vortex filamentation: its onset and its role on axisymmetrization and merger. *Dyn. Atmos. Oceans* **40** (1–2), 23–42.
- XIAO, Z., WAN, M., CHEN, S. & EYINK, G.L. 2009 Physical mechanism of the inverse energy cascade of two-dimensional turbulence: a numerical investigation. *J. Fluid Mech.* **619**, 1–44.
- YASUDA, I. & FLIERL, G.R. 1997 Two-dimensional asymmetric vortex merger: merger dynamics and critical merger distance. *Dyn. Atmos. Oceans* **26** (3), 159–181.